UNIVERSITÄTSKLINIKUM HAMBURG-EPPENDORF

III. Medizinische Klinik

Prof. Dr. Tobias B. Huber

IL-9 schützt vor frühem Podozytenschaden und progressiver Glomerulosklerose in der murinen Adriamycin-induzierten Nephropathie

Dissertation

zur Erlangung des Grades eines Doktors der Medizin
an der Medizinischen Fakultät der Universität Hamburg.

vorgelegt von:

Madena Attar
aus Hamburg

Hamburg 2022

Angenommen von der
Medizinischen Fakultät der Universität Hamburg am: 25.04.2023

Veröffentlicht mit Genehmigung der
Medizinischen Fakultät der Universität Hamburg.

Prüfungsausschuss, der/die Vorsitzende: **Prof. Dr. Gisa Tiegs**

Prüfungsausschuss, zweite/r Gutachter/in: **PD Dr. Jan-Eric Turner**

Inhaltsverzeichnis

Interleukin-9 protects from early podocyte injury and progressive glomerulosclerosis in Adriamycin-induced nephropathy

see commentary on page 541

Tingting Xiong[1,8], Madena Attar[1,8], Ann-Christin Gnirck[1], Malte Wunderlich[1], Martina Becker[1], Constantin Rickassel[1], Victor G. Puelles[1], Catherine Meyer-Schwesinger[2], Thorsten Wiech[3], Jasper F. Nies[1], Mylène Divivier[4], Tobias Fuchs[4], Julian Schulze zur Wiesch[5], Hanna Taipaleenmäki[6], Elion Hoxha[1], Stefan Wirtz[7], Tobias B. Huber[1], Ulf Panzer[1] and Jan-Eric Turner[1]

[1]*III. Department of Medicine, University Medical Center Hamburg-Eppendorf, Hamburg, Germany;* [2]*Department of Cellular and Integrative Physiology, University Medical Center Hamburg-Eppendorf, Hamburg, Germany;* [3]*Institute of Pathology, Nephropathology Section, University Medical Center Hamburg-Eppendorf, Hamburg, Germany;* [4]*Institute of Clinical Chemistry and Laboratory Medicine, University Medical Center Hamburg-Eppendorf, Hamburg, Germany;* [5]*I. Department of Medicine, University Medical Center Hamburg-Eppendorf, Hamburg, Germany;* [6]*Department of Trauma, Hand and Reconstructive Surgery, University Medical Center Hamburg-Eppendorf, Hamburg, Germany; and* [7]*Department of Internal Medicine 1, Friedrich Alexander University Erlangen-Nürnberg, University Medical Center Erlangen, Erlangen, Germany*

A wide spectrum of immunological functions has been attributed to Interleukin 9 (IL-9), including effects on the survival and proliferation of immune and parenchymal cells. In recent years, emerging evidence suggests that IL-9 expression can promote tissue repair in inflammatory conditions. However, data about the involvement of IL-9 in kidney tissue protection is very limited. Here, we investigated the role of IL-9 in Adriamycin-induced nephropathy (AN), a mouse model for proteinuric chronic kidney disease. Compared to wild type mice, IL-9 knockout (*Il9*$^{-/-}$) mice with AN displayed accelerated development of proteinuria, aggravated glomerulosclerosis and deterioration of kidney function. At an early stage of disease, the *Il9*$^{-/-}$ mice already displayed a higher extent of glomerular podocyte injury and loss of podocyte number compared to wild type mice. In the kidney, T cells and innate lymphoid cells produced IL-9. However, selective deficiency of IL-9 in the innate immune system in *Il9*$^{-/-}$*Rag2*$^{-/-}$ mice that lack T and B cells did not alter the outcome of AN, indicating that IL-9 derived from the adaptive immune system was the major driver of tissue protection in this model. Mechanistically, we could show that podocytes expressed the IL-9 receptor *in vivo* and that IL-9 signaling protects podocytes from Adriamycin-induced apoptosis *in vitro*. Finally, *in vivo* treatment with IL-9 effectively protected wild type mice from glomerulosclerosis and kidney failure in the AN model. The detection of increased serum IL-9 levels in patients with primary focal and segmental glomerulosclerosis further suggests that IL-9 production is induced by glomerular injury in humans. Thus, IL-9 confers protection against experimental glomerulosclerosis, identifying the IL-9 pathway as a potential therapeutic target in proteinuric chronic kidney disease.

Kidney International (2020) **98,** 615–629; https://doi.org/10.1016/j.kint.2020.04.036

KEYWORDS: cytokines; focal segmental glomerulosclerosis; inflammation; lymphocytes

Translational Statement

We show here that the type 2 cytokine interleukin-9 (IL-9) confers protection against experimental glomerulosclerosis by inhibiting early podocyte injury in Adriamycin-induced nephropathy. The detection of increased serum IL-9 levels in patients with primary focal segmental glomerulosclerosis further suggests that IL-9 production is induced by glomerular injury in humans. The potential therapeutic relevance of our finding is emphasized by IL-9 gene transfer experiments in which overexpression of IL-9 substantially ameliorated glomerulosclerosis and renal function impairment in the chronic kidney disease model.

Chronic kidney disease (CKD) is an increasing public health issue worldwide, leading to adverse outcomes that, in addition to possible progression to end-stage renal disease, include a significantly increased risk for cardiovascular mortality.[1] Numerous studies have revealed a crucial role of the immune system in driving renal tissue injury. However, regulatory components of the immune system can also promote resolution of kidney injury and restrain chronic inflammation.[2,3]

Correspondence: *Jan-Eric Turner, III. Department of Medicine, University Medical Center Hamburg-Eppendorf, Martinistrasse 52, D-20246 Hamburg, Germany. E-mail: j.turner@uke.de*

[8]TX and MA are co-first authors.

Received 22 May 2019; revised 29 March 2020; accepted April 2020; published online 21 May 2020

Cytokines play a central role in orchestrating tissue responses under both homeostatic and inflammatory conditions. Recent studies have highlighted an essential regulatory role of the cytokine interleukin-9 (IL-9) in autoimmune and chronic inflammatory diseases.[4] The production of IL-9 has been attributed to various cell types including T helper 2 (Th2),[4,5] Th17,[6] and regulatory T (Treg) cells.[7,8] In recent years, the existence of "Th9" cells, a Th subset that is dedicated to the production of IL-9, has also been proposed.[9,10] However, whether these cells represent a separate subset is still a matter of debate.[11] Apart from cells of the adaptive immune system, group 2 innate lymphoid cells (ILC2)[12,13] and mast cells[14] have also been identified as cellular sources of IL-9.

A wide spectrum of immunological functions has been attributed to IL-9, including the support of growth and survival of T cells and mast cells, as well as modulation of B cell responses.[15–18] Most of its diverse effects are exerted via direct regulation of immune cell function, but notably IL-9 can also act on nonimmune cells.[19–21] For a long period, the function of IL-9 has mainly been investigated in type 2 immune responses, while its role in autoimmune diseases and chronic tissue inflammation is less well characterized. A first indication that IL-9 might have a protective role in inflammatory conditions was provided by a study demonstrating that ILC2-derived IL-9 can promote tissue repair in helminth-induced acute lung injury.[13] In line with this finding, a more recent study showed that IL-9 deficiency prevents resolution of joint swelling in an arthritis model, while overexpression of IL-9 accelerated resolution of chronic inflammation.[22] In contrast to these protective effects of IL-9 in inflammatory lung injury and arthritis, a previous report indicated a proinflammatory role of IL-9 in inflammatory bowel disease.[20] Moreover, IL-9 has been linked to accelerated development of atherosclerosis[23,24] and vein graft disease,[25] pointing to a complex role of IL-9 in settings of autoimmunity, chronic inflammation, and tissue remodeling.

The exact cellular sources and functions of IL-9 in immune-mediated kidney diseases have not been examined in detail so far. While 2 studies suggest that IL-9 is involved in renal tissue protection in models of glomerulonephritis[7] and ischemia-reperfusion injury,[26] a recent investigation contradicted these findings by demonstrating that long-term IL-9 application can promote renal collagen deposition.[27]

In this study, we investigated the role of IL-9 in AN, a mouse model of proteinuric CKD and show that IL-9 deficiency leads to increased podocyte damage, aggravated glomerulosclerosis, and impairment of renal function. Moreover, IL-9 overexpression by hydrodynamic gene transfer effectively protected from progressive glomerulosclerosis and kidney failure. We further show that podocytes express the IL-9 receptor (IL-9R) *in vivo* and that IL-9 signaling protects podocytes from Adriamycin-induced apoptosis. In summary, we show here that IL-9 contributes to renal tissue protection in AN, identifying it as a potential therapeutic target in proteinuric CKD.

RESULTS

IL-9 protects from progressive glomerulosclerosis and renal failure in AN

To investigate the potential role of IL-9 in proteinuric CKD, we induced AN, a standard model for progressive glomerulosclerosis,[28] in BALB/c $Il9^{-/-}$ mice and wild-type (WT) controls. While naïve WT and $Il9^{-/-}$ mice showed only minimal levels of albuminuria that were not different between the 2 groups, albuminuria was significantly higher in $Il9^{-/-}$ mice, as compared to their WT counterparts, at an early stage of Adriamycin-induced nephropathy (AN; day 7). However, with progression of renal disease proteinuria in WT mice increased to the level observed in $Il9^{-/-}$ mice (Figure 1a). Importantly, histopathological examination of periodic acid–Schiff (PAS)-stained kidney sections revealed significantly aggravated glomerulosclerosis in $Il9^{-/-}$ mice at day 14, while the tubulointerstitial damage did not differ compared with that of WT mice (Figure 1b and c). Consistent with more pronounced glomerular damage, $Il9^{-/-}$ mice also displayed significantly higher levels of blood urea nitrogen (BUN) at day 14, indicating severe impairment of kidney function (Figure 1d). Cholesterol level, a marker for severity of the nephrotic syndrome, did not differ between the 2 groups (Figure 1e).

Taken together, these findings demonstrate that IL-9 deficiency leads to increased proteinuria at an early stage of AN, resulting in aggravated glomerulosclerosis and severe renal function impairment as the disease progresses.

IL-9 deficiency does not influence immune cell infiltration into the kidney and Treg phenotype in kidney and renal lymph nodes

It has become increasingly clear that infiltration of immune cells plays a key role in the pathogenesis of glomerular diseases and renal tissue injury leading to progression of CKD.[29] As IL-9 has been shown to affect various immune cell populations,[11] we first examined whether IL-9 deficiency modifies immune cell infiltration into the kidney. Flow cytometric analyses of cellular infiltrates in $Il9^{-/-}$ and WT mice after induction of AN revealed similar accumulation of $CD4^+$ T cells, $CD8^+$ T cells, Tregs, and ILC2s in $Il9^{-/-}$ and WT mice. Similarly, IL-9 deficiency did not influence infiltration of myeloid cell subsets, such as neutrophils, eosinophils, and mononuclear phagocytes (Supplementary Figure S1A and B). Tregs from $Il9^{-/-}$ mice have been shown to express reduced levels of coinhibitory molecules, such as glucocorticoid-induced tumor necrosis factor receptor family related protein (GITR) and inducible T cell costimulator (ICOS).[22] Moreover, IL-9–deficient Tregs have a reduced suppressive capacity in mouse models of glomerulonephritis[7] and rheumatoid arthritis.[22] To address the impact of IL-9 deficiency on Treg phenotype in the AN model, we compared expression of ICOS, GITR, and of programmed cell death protein 1 on Tregs from the renal lymph node and kidney of WT and $Il9^{-/-}$ mice under homeostatic conditions and at day 14 after induction of AN. However, we were unable to detect differences

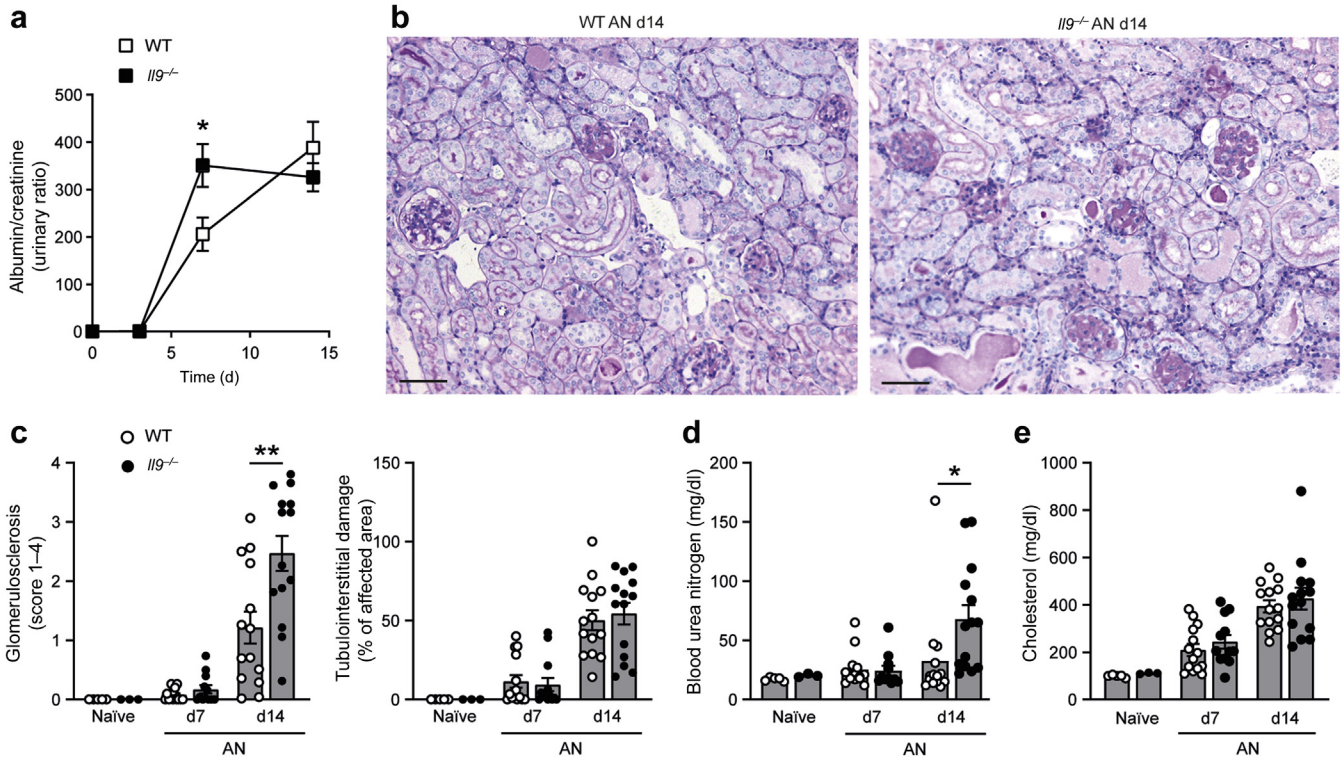

Figure 1 | *Il9*$^{-/-}$ mice show an aggravated phenotype in Adriamycin-induced nephropathy (AN). (**a**) Quantification of proteinuria, (**b**) representative photographs of periodic acid–Schiff–stained kidney sections (original magnification ×400; bars = 100 μm), (**c**) histopathological quantification of glomerular and interstitial damage, and analysis of (**d**) blood urea nitrogen, as a renal function parameter, and (**e**) cholesterol level, as a marker of severity of nephrotic syndrome, in naïve mice, as well as in BALB/c wild-type (WT) and *Il9*$^{-/-}$ mice at day 7 (d7) and day 14 (d14) after induction of Adriamycin nephropathy (naïve WT controls, $n = 5$; naïve *Il9*$^{-/-}$ controls, $n = 3$; WT d7, $n = 14$; WT d14, $n = 14$; *Il9*$^{-/-}$ d7, $n = 11$–12; *Il9*$^{-/-}$ d14, $n = 14$). (**a**) Symbols and (**c**–**e**) bars represent mean ± SEM. Open and filled circles represent individual animals. Data are pooled from 2 individual experiments with similar results. *$P < 0.05$, **$P < 0.01$.
To optimize viewing of this image, please see the online version of this article at www.kidney-international.org.

in coinhibitory protein expression on WT and *Il9*$^{-/-}$ Tregs in both tissues of naïve and diseased mice (Supplementary Figure S2A and B). In summary, we could not detect alterations in the immune cell infiltrate in the kidney and in Treg phenotype in the kidney and renal lymph nodes of *Il9*$^{-/-}$ mice in AN.

IL-9 does not protect from glomerular injury in experimental crescentic glomerulonephritis

To address the question whether IL-9 contributes to renal tissue protection in immune-mediated glomerular injury, we analyzed the phenotype of *Il9*$^{-/-}$ mice in a model of crescentic glomerulonephritis (nephrotoxic nephritis [NTN]) (Supplementary Figure S3). Histopathological examination of PAS-stained kidney sections and albuminuria in WT and *Il9*$^{-/-}$ mice at day 11 after induction of NTN did not reveal significant differences in glomerular or tubulointerstitial damage between the 2 groups (Supplementary Figure S3A–C). However, nephritic *Il9*$^{-/-}$ mice showed a small but significant increase in BUN levels as compared to that of their WT counterparts. This demonstrates that the protective IL-9 effect on glomerular injury developing as a result of direct podocyte injury by Adriamycin (Cell Pharm GmbH, Hannover, Germany) is less relevant in a primarily immune-mediated model, such as NTN.

IL-9 protects from early podocyte injury in AN

To determine the morphological correlate for elevated albuminuria in *Il9*$^{-/-}$ mice at early stages of AN, we assessed podocyte damage by electron microscopy at day 7, a time point where glomeruli appear largely normal in standard light microscopy. These analyses revealed a significantly higher extent of podocyte foot process effacement in *Il9*$^{-/-}$ mice at day 7 of AN (Figure 2a and b). In addition, quantification of total podocytes in the glomeruli of WT and *Il9*$^{-/-}$ mice via immunohistochemical staining at day 7 of AN revealed a significant reduction in podocyte numbers in *Il9*$^{-/-}$ mice (Figure 2c and d). Of note, there was no difference in podocyte number and foot process structure between WT and *Il9*$^{-/-}$ mice at steady state (Figure 2a and d). Taken together, these data point to a role of IL-9 in protecting podocytes from Adriamycin-induced injury and cell loss in early stages of AN.

T cells and ILCs are the main cellular sources of IL-9 in AN

To characterize cellular sources of IL-9 in progressive CKD, we induced AN in *Il9*^{Cre}*R26R*^{tdtomato} "fate reporter" mice, in

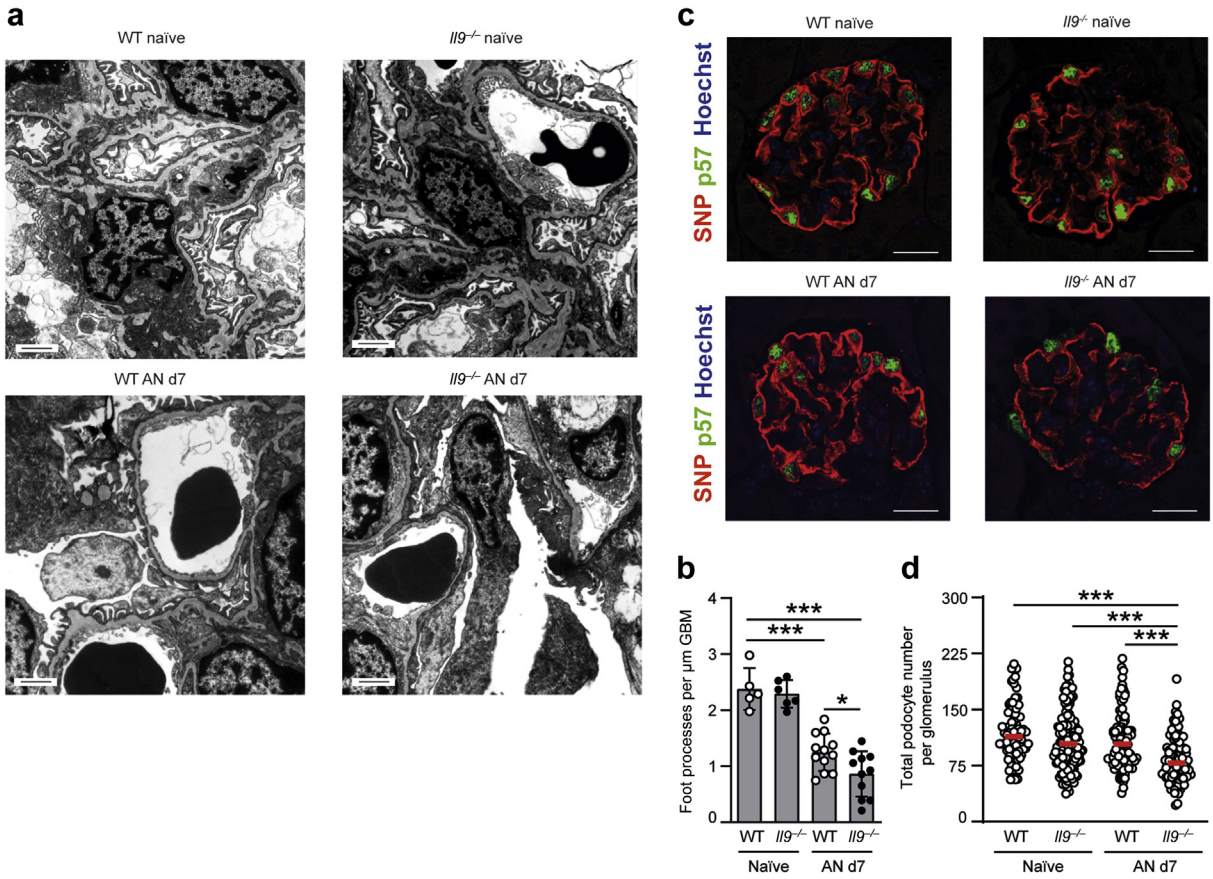

Figure 2 | Early podocyte damage is aggravated in *Il9*$^{-/-}$ mice in Adriamycin-induced nephropathy (AN). (**a**) Representative electron microscopy of podocytes and (**b**) quantification of podocyte foot processes in naïve wild-type (WT) and *Il9*$^{-/-}$ mice, as well as in WT and *Il9*$^{-/-}$ mice at day 7 (d7) after induction of AN (naïve WT controls, $n = 5$; naïve *Il9*$^{-/-}$, $n = 5$; WT d7, $n = 12$; *Il9*$^{-/-}$ d7, $n = 11$). Bars = 1000 nm and represent mean ± SEM. Circles represent individual animals. (**c**) Representative immunohistochemical staining of podocytes and (**d**) quantification of total podocyte number per glomerulus in naïve WT and *Il9*$^{-/-}$ mice, as well as in WT and *Il9*$^{-/-}$ mice at d7 after induction of AN ($n = 100$ with each dot representing 1 glomerulus; 5 mice with 20 glomeruli per mouse were analyzed in each group). Bars = 20 µm. Symbols represent podocyte number per individual glomerulus with the horizontal red line representing the median. Data are pooled from 2 individual experiments with similar results. *$P < 0.05$, ***$P < 0.001$. GBM, glomerular basement membrane; SNP, synaptopodin. To optimize viewing of this image, please see the online version of this article at www.kidney-international.org.

which cells that have expressed IL-9 are permanently marked by the fluorescent protein td-tomato, further referred as IL-9 "fate mapped" (IL-9^{fm+}) cells. Immunohistochemical detection of the td-tomato protein in kidney sections of naïve and diseased *Il9*^{Cre}*R26R*^{tdtomato} mice revealed IL-9^{fm+} cells that were located in the glomeruli, the tubulointerstitial infiltrates, and the perivascular spaces (Figure 3a). Flow cytometric analyses of leukocytes isolated from the kidney of nephritic mice at day 14 of AN and from naïve controls showed a low but constant expression of IL-9 in CD45^{+} lymphocytes (Figure 3b), while IL-9 expression in renal nonlymphoid leukocytes and CD45-negative nonhematopoietic cells was virtually absent (Supplementary Figure S4A). Moreover, we did not detect a substantial number of IL-9^{fm+} cells in peripheral blood mononuclear cells or in the spleen of naïve or diseased mice (Supplementary Figure S4B and C). A more detailed analysis revealed that CD90.2^{+}CD3^{-} lineage marker-negative ILCs and CD4^{+} T cells were the major cellular sources of IL-9 in naïve and nephritic mice (Figure 3c and d), while the percentage of IL-9^{fm+} CD4^{+} T cells and ILCs was unchanged during disease progression (Figure 3d). As described before,[12] IL-9 production in naïve T cells can be stimulated by T cell receptor (TCR) activation in conjunction with a combination of cytokines (transforming growth factor-β, IL-4, IL-6, IL-1β) (Supplementary Figure S5A). Although IL-9 reporter-positive T cells in the kidney did not significantly increase in numbers during the course of AN, we could show that IL-9 production in kidney effector T cells could be stimulated by TCR activation and the above-mentioned combination of cytokines that, with the exception of IL-4, are upregulated in the kidneys of AN mice (Supplementary Figure S5B and C). These data provide a potential mechanism of how T cells residing in the kidney of naïve mice could be stimulated to release IL-9 in the inflammatory setting of AN.

IL-9 from the adaptive immune system is required for its protective effect in AN

Because ILCs were the most abundant IL-9^{fm+} cell subset in the kidney (see Figure 3c), we next addressed the hypothesis

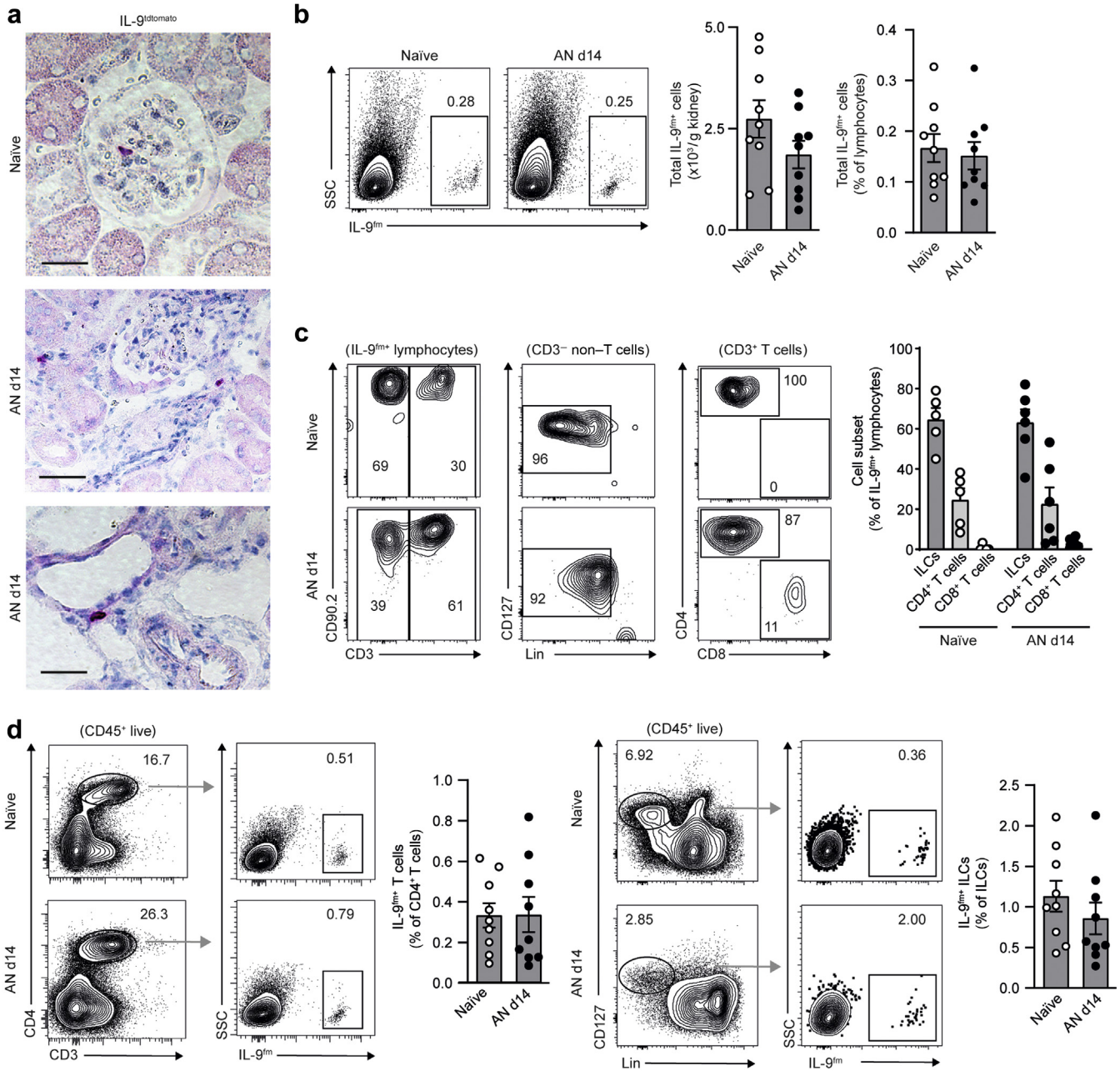

Figure 3 | T cells and innate lymphoid cells (ILCs) are major cellular sources of interleukin-9 (IL-9) in the kidney. (**a**) Representative immunohistochemistry of kidney sections of naïve and diseased *Il9*^{Cre}*R26r*^{tdtomato} fate reporter mice for the td-tomato protein (original magnification ×400; bars = 25 μm). (**b**) Representative flow cytometry analysis and quantification of IL-9 fate-mapped (IL-9^{fm+} = td-tomato–positive) cells in the kidneys of naïve and diseased *Il9*^{Cre}*R26r*^{tdtomato} mice at day 14 (d14) of Adriamycin-induced nephropathy (AN). (**c**) Representative flow cytometry analyses and quantification of T cell– (mostly CD4^{+} T cells) and non–T cell–frequencies (mostly CD127^{+} lineage marker [Lin]–negative ILCs) among renal IL-9^{fm+} cells. (**d**) Percentage of IL-9^{fm+} CD4^{+} T cells and IL-9^{fm+} ILCs in the kidney with the corresponding quantifications. Gating strategy is specified in parentheses, and numbers indicate the percentage of cells in the respective gates. (**b–d**) Bars represent mean ± SEM (naïve controls, n = 5–9; AN d14, n = 5–9). Open and filled circles represent individual animals. Data are pooled from (**c**) 2 or (**b,d**) 3 individual experiments with similar results. SSC, side scatter. To optimize viewing of this image, please see the online version of this article at www.kidney-international.org.

that IL-9 from the innate immune system (e.g., ILCs) plays a decisive role in protection from experimental glomerulosclerosis. To this end, we backcrossed *Il9*$^{-/-}$ mice to a *Rag2*$^{-/-}$ background, lacking T and B cells, and compared them with IL-9–competent *Rag2*$^{-/-}$ mice, in which the innate immune system (including ILCs) is capable of producing IL-9 in absence of an adaptive source of IL-9 (e.g., CD4^{+} T cells). These analyses revealed a similar degree of glomerulosclerosis at day 14 after induction of AN in *Rag2*$^{-/-}$ and *Rag2*$^{-/-}$*Il9*$^{-/-}$ mice (Figure 4a and b). In line, analyses of kidney function

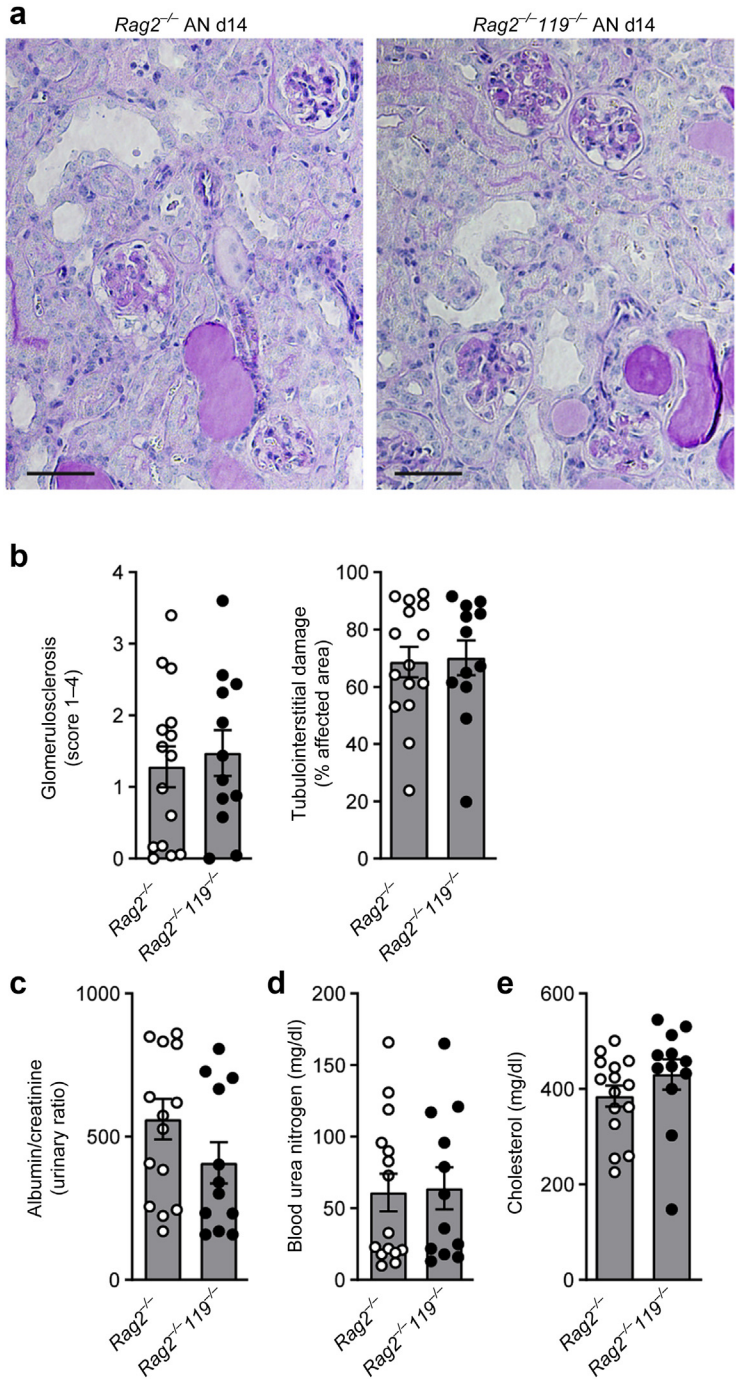

Figure 4 | *Rag2*$^{-/-}$*Il9*$^{-/-}$ mice do not show aggravation of renal damage in Adriamycin-induced nephropathy (AN). (**a**) Representative photographs of periodic acid–Schiff–stained kidney sections (original magnification ×400; bars = 100 μm), (**b**) histopathological quantification of glomerular and interstitial damage, and (**c–e**) analysis of proteinuria, blood urea nitrogen, and cholesterol level in *Rag2*$^{-/-}$ and *Rag2*$^{-/-}$*Il9*$^{-/-}$ mice at day 14 (d14) after induction of AN (*Rag2*$^{-/-}$, $n = 15$; *Rag2*$^{-/-}$*Il9*$^{-/-}$, $n = 12$). (**b–e**) Bars represent mean ± SEM. Open and filled circles represent individual animals. Data are pooled from 2 individual experiments with similar results. To optimize viewing of this image, please see the online version of this article at www.kidney-international.org.

parameters were similar between the 2 groups (Figure 4c–e). Collectively, these findings suggest that T-cell–derived IL-9 plays an important role for protection from glomerulosclerosis, while IL-9 produced by the innate immune system seems to be dispensable for control of renal injury in AN.

IL-9 protects podocytes from Adriamycin-induced cell death

IL-9 is believed to exert most of its effects via direct regulation of immune cell function,[11] but it has also been demonstrated that IL-9 can have direct antiapoptotic effects on nonimmune cells.[19,20,30] Because we were unable to

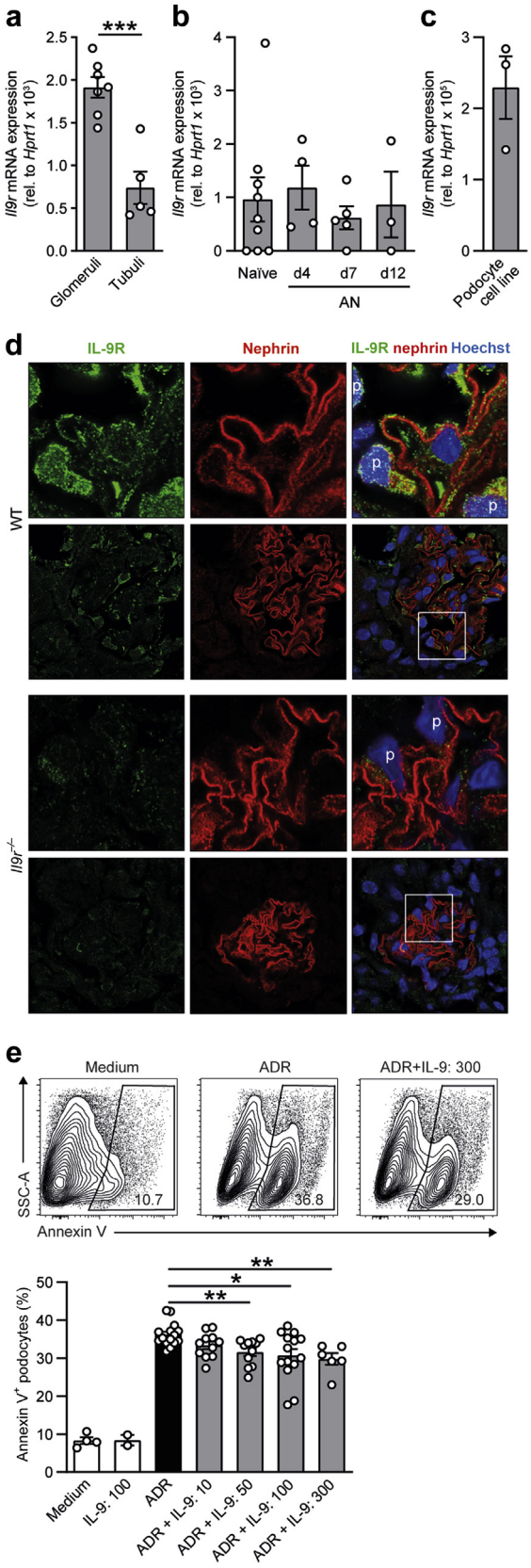

Figure 5 | Intereukin-9 (IL-9) protects podocytes from Adriamycin-induced cell death. (**a**) Quantitative real-time polymerase chain reaction analysis of IL-9 receptor (IL-9R) mRNA expression in the glomerular and tubular compartment (continued)

detect a substantial impact of IL-9 deficiency on the immune cell compartment (see Supplementary Figures S1 and S2), we hypothesized that IL-9 might mediate its tissue protective effect in AN by directly acting on renal epithelial cells. To identify potential targets of IL-9 signaling in the kidney, we assessed *Il9r* mRNA expression in isolated glomerular and tubulointerstitial compartments from naïve WT mice. Interestingly, *Il9r* mRNA expression level in the glomerular compartment was readily detectable and markedly higher than in the tubulointerstitial compartment (Figure 5a). Furthermore, real-time polymerase chain reaction (PCR) analysis showed an unaltered mRNA expression level of the IL-9R in the glomerular compartment during the course of AN (Figure 5b). Because, among glomerular cells, podocytes represent the main target of Adriamycin-induced injury, we next performed real-time PCR analysis for the IL-9R on a murine podocyte cell line, demonstrating relevant expression of *Ill9r* mRNA (Figure 5c). To provide *in vivo* evidence for IL-9R expression on podocytes, we performed IL-9R immunofluorescence staining on kidney sections of WT and $Il9r^{-/-}$ mice, as a negative control (Figure 5d). Indeed, these analyses demonstrated specific expression of the IL-9R on podocytes and, to a lesser extent, on glomerular endothelial cells (Figure 5d). To further explore the hypothesis that IL-9 protects from Adriamycin-induced glomerulosclerosis by directly regulating podocyte survival, we pretreated murine podocyte cell lines with recombinant IL-9 in increasing concentrations, followed by incubation with Adriamycin to induce podocyte apoptosis. Indeed, quantification of annexin V–positive podocytes showed a small but significant reduction of Adriamycin-induced podocyte apoptosis in cultures supplemented with IL-9 concentrations of 50 ng/ml and above (Figure 5e), indicating that IL-9 signaling might ameliorate glomerulosclerosis by preventing early podocyte death in the AN model.

Figure 5 | (continued) of the kidney in naïve wild-type (WT) mice (glomeruli, $n = 7$; tubuli, $n = 5$). (**b**) Quantitative real-time polymerase chain reaction analysis of IL-9R mRNA expression in the glomerular compartment of WT mice at day 4 (d4), day 7 (d7), and day 12 (d12) after induction of Adriamycin-induced nephropathy ([AN]; naïve WT control, $n = 9$; WT d4, $n = 4$; WT d7, $n = 5$; WT d12, $n = 3$). (**c**) Quantitative real-time polymerase chain reaction analysis of IL-9R mRNA expression in a murine podocyte cell line ($n = 3$). (**d**) Representative immunohistochemical staining of IL-9R in naïve WT and $Il9r^{-/-}$ mice (p indicates podocytes). (**e**) Representative flow cytometry plots of murine podocytes treated with medium only, Adriamycin (ADR), or ADR + IL-9 (300 ng/ml), and quantification of dead podocytes (medium, $n = 4$; IL-9, $n = 2$; ADR, $n = 15$; ADR + IL-9, $n = 11$–14 per concentration). Numbers indicate the percentage of cells in the gates. (**a–c,e**) Bars represent mean ± SEM. Open and filled circles represent individual data points. (**e**) Data are pooled from 3 individual experiments with similar results. $^{*}P < 0.05$, $^{**}P < 0.01$, $^{***}P < 0.001$. rel, relative; SSC-A, side scatter area. To optimize viewing of this image, please see the online version of this article at www.kidney-international.org.

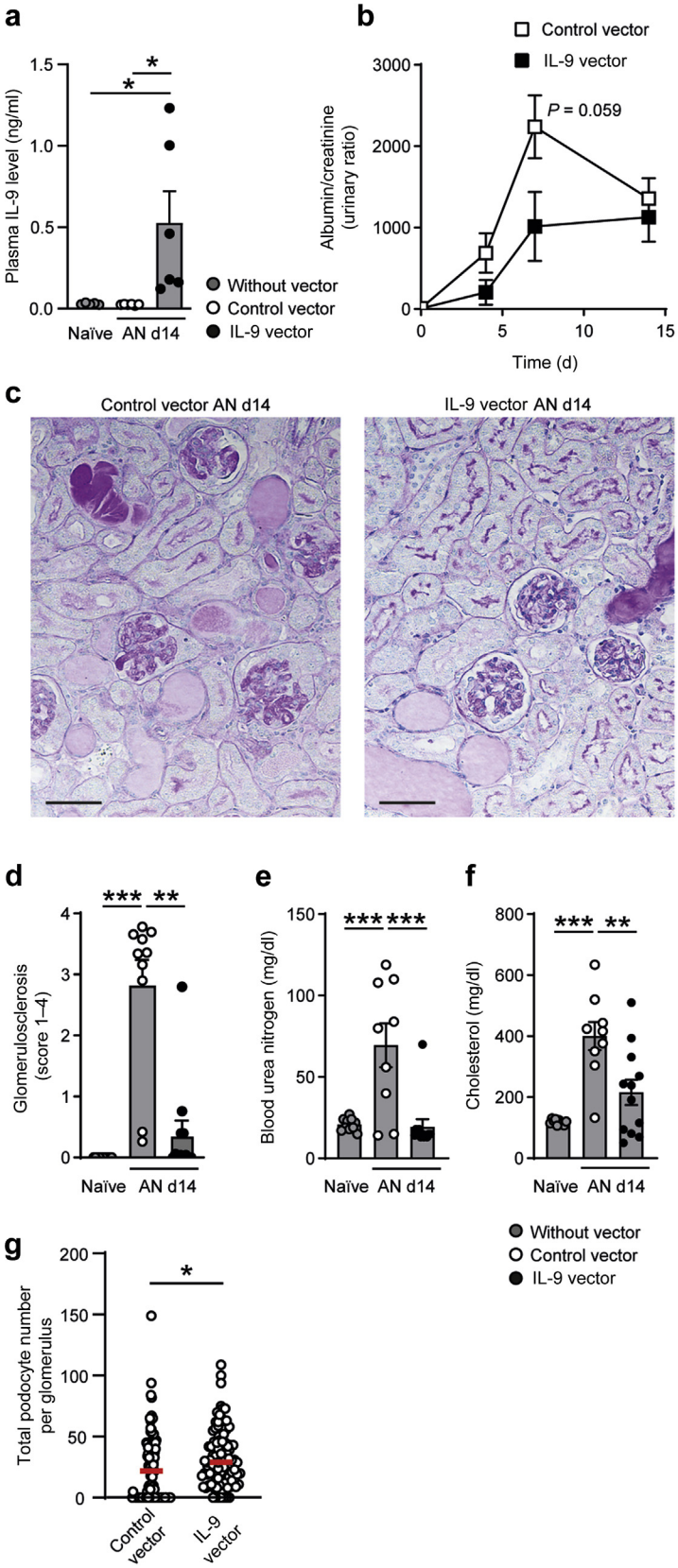

Figure 6 | Interleukin-9 (*Il9*) gene transfer ameliorates renal outcome in Adriamycin-induced nephropathy (AN). (**a**) Quantification of IL-9 plasma levels in naïve mice and in BALB/c wild-type mice at day 14 (d14) of AN, treated with control vector or IL-9 vector 3 days prior to induction of the model. Data are representative for 2 individual experiments with similar results, 1 of which showed IL-9 levels that (continued)

IL-9 treatment protects from glomerulosclerosis and kidney failure

IL-9 has previously been described to promote tissue repair in lung injury and resolution of inflammation in arthritis.[13,22] To assess the therapeutic potential of IL-9 to ameliorate progressive glomerulosclerosis and kidney failure *in vivo,* we induced overexpression of IL-9 in the liver by hydrodynamic gene transfer, using minicircle vectors encoding IL-9, 3 days prior to injection of Adriamycin. Indeed, mice treated with the IL-9 vector had significantly increased plasma IL-9 levels (Figure 6a) and showed lower levels of albuminuria, albeit the latter was not significant (Figure 6b). Remarkably, mice treated with the IL-9 vector, compared with mice treated with the control vector, displayed a striking reduction in glomerular sclerosis (Figure 6c and d). Consistently, IL-9–treated mice showed marked lower levels of BUN (Figure 6e) and cholesterol, as a marker of the nephrotic syndrome (Figure 6f). Furthermore, quantification of podocytes at day 14 of AN revealed a significant reduction in podocyte loss in mice treated with the IL-9 vector (Figure 6g).

In summary, our findings clearly show that IL-9 deficiency leads to aggravated glomerular sclerosis and impaired renal function, whereas overexpression of IL-9 *in vivo* significantly ameliorates renal histological and functional outcomes in AN.

IL-9 is upregulated in the serum of patients with primary focal segmental glomerulosclerosis (FSGS)

To strengthen the relevance of our findings for human kidney disease, we analyzed serum samples of healthy controls and of patients with primary FSGS, a disease in which direct podocyte injury of yet unknown origin results in foot process effacement, nephrotic proteinuria, and subsequent glomerulosclerosis.[31] The characteristics of patients and healthy controls are given in Supplementary Table S1. By using a highly sensitive immunoassay, we were able to detect IL-9 in all samples. Most importantly, IL-9 levels were significantly increased in patients with primary FSGS (Figure 7), which is consistent with the hypothesis that glomerular injury leads to upregulation of IL-9. Because we were not able to detect a significant correlation of IL-9 levels with proteinuria ($r = 0.178$) or creatinine ($r = 0.525$) in this small patient cohort, further investigation will be needed to explore a potential functional meaning of increased IL-9 levels in human primary FSGS. Of note, the control cohort was significantly younger than the patient cohort (43 ± 3 years vs. 55 ± 4 years; $P = 0.024$). However, there was no correlation of age with IL-9 levels in patients with FSGS ($r = 0.222$) or controls ($r = -0.370$).

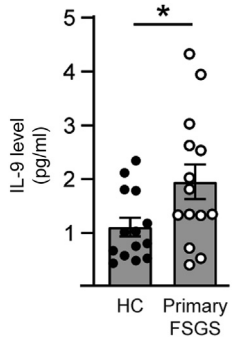

Figure 7 | Serum interleukin-9 (IL-9) level is increased in patients with primary focal segmental glomerulosclerosis (FSGS). IL-9 level in serum samples of healthy controls (HCs) and patients with primary FSGS. Bars represent mean ± SEM (HCs, $n = 14$; primary FSGS, $n = 14$). Circles represent individual patients. *$P < 0.05$.

DISCUSSION

CKD is a global health burden, affecting around 10% of the population in industrialized countries and is strongly associated with increased cardiovascular mortality.[1] Despite considerable progress that has been made in this field of research, current treatment options for CKD are still very limited, and further elucidation of the pathways regulating its progression is required to enable development of novel therapeutics. Several recent studies indicate that, following infection or sterile injury, the type 2 immune response can activate crucial repair pathways that help to restore tissue integrity. Type 2 immunity has thus been identified as a promising therapeutic target in CKD[32–35] and other chronic inflammatory conditions.[36–38] Type 2 immune responses are characterized by production of IL-4, IL-5, IL-9, and IL-13 by $CD4^+$ T cells and ILC2s that orchestrate a complex immune cell network, involving eosinophils, mast cells, basophils, and alternatively activated macrophages.[36] While the role of the cytokine IL-9 in "classical" type 2 responses, such as allergic diseases and helminth infections, has been extensively investigated, a potential role of IL-9 in chronic tissue inflammation and regeneration is only beginning to be unraveled.

Figure 6 | (continued) exceeded the upper detection threshold of the enzyme-linked immunosorbent assay in the IL-9 vector–treated group and is, therefore, not shown here. (**b**) Quantification of albuminuria at days 4, 7, and 13 after induction of AN ($n = 8$–12 per group). (**c**) Representative photographs of periodic acid–Schiff–stained kidney sections (original magnification ×400; bars = 100 μm), (**d**) histopathological quantification of glomerular damage, and analysis of (**e**) blood urea nitrogen, and (**f**) cholesterol level in the 3 groups ($n = 10$–12 per group). (**a,b,d–f**) Bars represent mean ± SEM. Open and filled circles represent individual animals. (**b,d–f**) Data are pooled from 2 experiments with similar results. (**g**) Quantification of total podocyte number per glomerulus in BALB/c wild-type mice at d14 of AN, treated with control vector or IL-9 vector 3 days prior to induction of the model ($n = 100$ with each dot representing 1 glomerulus; 5 mice with 20 glomeruli per mouse were analyzed in each group). Symbols represent podocyte number per individual glomerulus with the horizontal red line representing the median. *$P < 0.05$, **$P < 0.01$, ***$P < 0.001$. To optimize viewing of this image, please see the online version of this article at www.kidney-international.org.

In the present study, we observe that IL-9 deficiency leads to acceleration of podocyte damage and glomerulosclerosis with severe impairment of renal function in Adriamycin-induced proteinuric CKD. We further demonstrate that the IL-9R is expressed on podocytes and that IL-9 signaling can have a direct antiapoptotic effect on this cell type, providing a potential mechanism for IL-9–mediated renal tissue protection. Remarkably, therapeutic overexpression of IL-9 *in vivo* effectively prevented progressive glomerulosclerosis and kidney failure in the CKD model.

First evidence that IL-9 can exert favorable effects on tissue regeneration was provided by a study demonstrating that, after helminth-induced lung injury, IL-9 can promote tissue repair by inducing the survival and activation of pro-regenerative ILC2s.[13] This concept of an IL-9–mediated tissue protective effect was further supported by a recent investigation in an arthritis model, indicating that the absence of IL-9 prevents spontaneous resolution of joint swelling, while overexpression of IL-9 via gene transfer attenuates arthritis in *Il9*$^{-/-}$ mice.[22] In line, a prior study demonstrated that absence of IL-9 signaling leads to worsening of experimental autoimmune encephalomyelitis,[39] a mouse model of multiple sclerosis. In arthritis and experimental autoimmune encephalomyelitis, the lack of IL-9 essentially impaired the suppressive activity of Treg cells, resulting in increased effector T cell responses and exacerbation of immune-mediated tissue damage. However, conflicting results have been reported by other investigators, demonstrating that IL-9 blockade by neutralizing antibodies or by IL-9R deficiency can ameliorate experimental autoimmune encephalomyelitis by attenuation of the Th17 response,[6,40] which points to a highly context-dependent role of IL-9 in neuroinflammation. While these studies provided evidence that IL-9 mediates its effect in lung injury, arthritis, and neuroinflammation, primarily by acting on immune cell activation and survival, a recent report showed that IL-9 can exert proinflammatory effects in inflammatory bowel disease by directly regulating expression of tight junction proteins in epithelial cells. Hence, in the intestine, IL-9 expression resulted in impaired intestinal barrier function and deterioration of mucosal wound healing capacity in a colitis model.[20] Taken together, these data suggest a complex and organ-specific role for IL-9 in regulation of tissue inflammation.

The implication of IL-9 signaling in kidney diseases is still incompletely understood. Here, we report that IL-9 effectively protects from glomerulosclerosis and renal function impairment in the AN model of CKD. Our results are in line with a previous report,[7] showing a beneficial IL-9–dependent effect of Tregs in an experimental model of crescentic glomerulonephritis. In this study, transfer of IL-9–competent CD4$^+$CD25$^+$ Tregs to nephritic mice was protective, while Treg cells from *Il9*$^{-/-}$ animals were not. The anti-inflammatory effect of Tregs was attributed to an attraction of immunosuppressive mast cells into the kidney draining lymph nodes. However, the question whether Tregs actually produced IL-9 in this setting, or whether Tregs from an IL-9–deficient environment are generally impaired in their immunosuppressive capacity, as suggested by the previously mentioned arthritis study,[22] was not addressed in this study. In the present study, we did not observe differences in number and phenotype of Tregs in kidney and renal lymph nodes, but we found a substantial effect of IL-9 deficiency on non–immune-mediated podocyte damage and loss at an early time point of AN (day 7). At this time point, the immune cell infiltration into the kidney is still minimal,[28] and it can be assumed that the impact of Treg cells (in the kidney or renal lymph node) on early Adriamycin-induced podocyte damage is limited. Furthermore, we did not observe a substantial effect of IL-9 deficiency in a primarily immune-mediated model of crescentic glomerulonephritis in which immune events in renal lymph nodes is far more important than in a model that is based on drug-induced direct podocyte injury, such as AN. Taken together, the data provided here support the hypothesis of a direct action of IL-9 on podocytes as a major driver of glomerular protection in the AN model. However, we cannot fully exclude that dysregulation in Tregs or other immune cell populations not investigated in this study contribute to the aggravated phenotype of IL-9 deficiency in progressive glomerulosclerosis.

For many years, the production of IL-9 has mainly been attributed to Th2 cells,[5,41] while few studies suggested IL-9 production by other T cell subsets, such as Tregs[7,8] and Th17 cells.[6] More recently, the existence of a Th cell subset dedicated to the production of IL-9 (Th9 cells) has also been proposed,[9,10] and a role for these cells in immune-mediated diseases has been suggested.[4] However, *in vivo* evidence for specialized Th9 cells is still inconclusive,[11] and in lung inflammation[12,13] and arthritis,[22] ILC2s have been determined as the predominant cellular source of IL-9 *in vivo*. In the present study, we used IL-9 fate reporter mice to identify and locate IL-9–producing cells *in vivo* and observed a low but continuous expression of IL-9 in the kidney during AN. Because IL-9–producing cells in the spleen and peripheral blood were very rare, it is likely that local IL-9 production in the kidney is responsible for the protective effect in AN. However, we show that systemic increase in IL-9 production induced by hydrodynamic gene transfer can prevent podocyte damage in AN, indicating that systemic IL-9 production can contribute to renal tissue protection. Although IL-9 in the kidney was produced by ILCs and CD4$^+$ T cells, our results indicate that IL-9 derived from the adaptive immune system plays a major role in conferring protection against glomerular injury induced by Adriamycin. The observed upregulation of IL-9 production in kidney effector CD4$^+$ T cells under the influence of cytokines and TCR stimulation *in vitro* provides a potential mechanism of how local IL-9 production in the kidney could be regulated.

Although it has been implicated that IL-9 can affect diverse immune cell subsets,[11] there is increasing evidence that apart from immune cells,[13] IL-9 has antiapoptotic effects on parenchymal cells, such as epithelial cells[30] and neurons.[19] The observation of exacerbated podocyte damage and pronounced

loss of podocyte numbers in *Il9*$^{-/-}$ mice at early stages of AN (a time point at which immune cell infiltration into the kidney is still minimal[28]), together with the absence of variations in renal leukocyte infiltrates in *Il9*$^{-/-}$ animals, prompted us to hypothesize that IL-9 might act directly on podocytes, representing the main target cells of Adriamycin-induced injury. In line with this hypothesis, we observed a distinct expression of the IL-9R on podocytes *in vivo* and in podocyte cell lines. Moreover, we could demonstrate a small but significant reduction of Adriamycin-induced podocyte apoptosis in cultures supplemented with IL-9. Potential mechanisms of antiapoptotic IL-9 effects include activation of the Janus kinase/signal transducer and activator of transcription pathway,[19] downregulation of the proapoptotic factor Bax,[19] as well as upregulation of the antiapoptotic proteins B cell lymphoma-2[19,30] and -3.[13] However, the antiapoptotic pathways that are activated by IL-9 signaling in podocytes were not in the focus of the present study and need to be further investigated in the future. The obvious discrepancy between the *in vivo* and *in vitro* sensitivity of podocytes to IL-9 might be explained by the fact that immortalized podocyte cell lines often poorly reflect receptor expression pattern and sensitivity to stimuli of podocytes *in vivo*. Thus, although our *in vivo* data suggest a distinct impact of IL-9 signaling in promoting podocyte survival in AN, we cannot exclude a potential contribution of other glomerular cell types, such as endothelial cells[42] that also showed a faint positivity for IL-9R in the immunohistochemistry (see Figure 5d), to the phenotype of IL-9 deficiency in the AN model.

A potential involvement of IL-9 in human kidney diseases has not been addressed in detail so far. However, a first study using a multiplex cytokine assay of urine samples from patients with anti-neutrophil cytoplasmic antibody–associated glomerulonephritis revealed that increased urinary excretion of IL-9 at the time of diagnosis might be correlated with a favorable outcome of renal function,[43] suggesting that IL-9 may contribute to renal tissue protection also in human glomerular diseases. Moreover, Kortekaas *et al.*[26] reported substantial IL-9 release from human kidney allografts during the first 30 minutes after reperfusion, indicating that IL-9 might be upregulated by ischemic renal injury in humans. In line with these results, we detected increased serum IL-9 levels in patients with primary FSGS, which is consistent with the hypothesis that glomerular injury leads to upregulation of IL-9 (with potential beneficial effects on podocyte survival). However, because we were not able to detect a significant correlation of IL-9 levels with clinical parameters in this small patient cohort, further investigation will be needed to explore a potential functional meaning of increased IL-9 levels in human primary FSGS.

The potential therapeutic relevance of our findings was further emphasized by the IL-9 gene transfer experiments in which overexpression of IL-9 almost completely prevented glomerulosclerosis and renal function impairment induced by Adriamycin, suggesting that IL-9–mediated protection of podocytes might also be functional *in vivo*. However, it is important to note in this context that a recent report contradicts a protective role of IL-9 in renal disease, by demonstrating that long-term IL-9 application (e.g., 40 days) promotes renal collagen deposition.[27] Moreover, several studies have linked chronically increased systemic IL-9 levels to aggravated development of atherosclerosis[23,24] and vein graft disease[25] and showed that anti-IL-9 treatment can confer vascular protection. Especially in light of a strong link between cardiovascular disease and CKD, these considerations are important in assessing the risk for potential side effects of long-term IL-9 therapy, which are likely to be determined by the dose, duration, and context of the cytokine exposure.

In conclusion, our results support a protective role of IL-9 in secondary progressive glomerulosclerosis and kidney failure induced by Adriamycin and suggest that overexpression of IL-9 ameliorates the renal outcome in this model by mediating an anti-apoptotic effect on podocytes. In principle, targeting the IL-9 pathway might represent a therapeutic option in proteinuric CKD. However, because IL-9 has also been linked to induction of fibrosis and aggravation of cardiovascular disease, further investigation of potential side effects of CKD therapies aimed at increasing IL-9 expression are warranted.

METHODS

Animals

WT *Il9*$^{-/-}$ (kindly provided by A. McKenzie, Cambridge, UK)[44] and *Rag2*$^{-/-}$ mice[45] were available on a BALB/c background. *Rag2*$^{-/-}$*Il9*$^{-/-}$ mice were generated by crossbreeding *Il9*$^{-/-}$ mice to *Rag2*$^{-/-}$ mice. *Il9*^{Cre}*R26R*^{tdtomato} mice (*Il9*^{Cre} mice kindly provided by B. Stockinger, London, UK)[12] and *Il9r*$^{-/-}$ (kindly provided by J.C. Renauld, Brussels, Belgium)[46] were backcrossed to the BALB/c background for 10 generations. All mice were bred in the animal facility of the University Medical Center Hamburg-Eppendorf under specific pathogen-free conditions. Adult male and female mice with their respective age- and sex-matched controls were used in all experiments. All animal experiments were performed according to national and institutional animal care and ethical guidelines and were approved by the local authorities.

Induction of progressive glomerulosclerosis, experimental glomerulonephritis, and functional studies

For induction of progressive glomerulosclerosis, BALB/c mice were injected i.v. with 12 μg Adriamycin (Cell Pharm) per gram body weight. Experimental crescentic glomerulonephritis (NTN) was induced by i.p. injection of nephrotoxic sheep serum (2.5 mg/g body weight) in 8 to 12-week-old mice as previously described.[47] For urine sample collection, mice were housed in metabolic cages for 5 hours. Urinary albumin excretion was determined by standard enzyme-linked immunosorbent assay (Mice-Albumin Kit; Bethyl Laboratories, Montgomery, TX). Urinary creatinine levels were measured with the Creatinine Jaffé Fluid (Hengler Analytik, Steinbach, Germany). Plasma cholesterol and BUN were analyzed by standard laboratory procedures.

Hydrodynamic gene transfer for induction of IL-9 overexpression

The principle of hydrodynamic gene transfer allowing for nonviral introduction of plasmid DNA into hepatocytes has been described in detail elsewhere.[48] Briefly, 10 μg of either IL-9 or control vector was

administered by tail vein injection in sodium chloride solution corresponding to 10% of mouse body weight. Progressive glomerulosclerosis was induced 72 hours after hydrodynamic gene transfer.

Cytokine measurements

IL-9 in mouse plasma was measured by enzyme-linked immunosorbent assay according to the manufacturer's instruction (BioLegend, San Diego, CA).

Histopathology, immunohistochemistry, and electron microscopy

Formalin-fixed, paraffin-embedded kidney sections were stained with PAS reagent according to standard laboratory procedures and assessed for histopathology in a blinded fashion. In AN, glomerular sclerosis was assessed by scoring deposition of PAS-positive material in 50 glomeruli per mouse from 0 to 4 (1 = 25% PAS-positive material, 2 = 50% PAS-positive material, 3 = 75% PAS-positive material, 4 = entirely sclerotic). The tubulointerstitial damage was assessed by superimposition of a grid onto nonoverlapping photographs of PAS-stained renal cortex cross sections. The percentage of area within the grid displaying dilated, atrophic, or cast-filled tubules was determined. In NTN, crescent formation was assessed in 30 glomeruli per mouse. The percentage of interstitial area, as a measure of tubulointerstitial cell infiltration and injury, was determined by using photographs of nonoverlapping cortical areas from PAS-stained kidney sections that were superimposed with 40 apportioned dots. Subsequently, interstitially located dots were counted and expressed as percentage of total dots. Scoring was performed with the Axioskop light microscope and photographs were taken with an Axiocam MRc camera (both ZEISS, Jena, Germany). For staining of IL-9–producing td-tomato–positive cells in $Il9^{Cre}R26R^{tdtomato}$ mice, paraffin sections of mouse kidneys were deparaffinized and rehydrated. Antigen retrieval was performed using a heat-induced method with Dako antigen retrieval buffer (Agilent Technologies, Santa Clara, CA) at pH 9. Nonspecific binding was blocked with 5% normal horse serum in phosphate-buffered serum (PBS) for 30 minutes at room temperature (RT) before incubation with the primary td-tomato antibody (orb182397; Biorbyt, St. Louis, MO) overnight at 4 °C. Next, sections were incubated with biotinylated rabbit anti-goat antibody (BA-5000; Vector Laboratories, Burlingame, CA) followed by incubation with anti-rabbit polymer (POLAP-006; Zytomed Systems, Berlin, Germany). Finally, sections were stained with neufuchsin and hemalaun. For immunohistochemical staining of total podocyte numbers, paraffin sections of mouse kidneys were deparaffinized and rehydrated. Antigen retrieval was performed using a heat-induced method with Dako antigen retrieval buffer at pH 9. Nonspecific binding was blocked with 1% bovine serum albumin in PBS for 30 minutes at RT before incubation with primary antibody made up in Dako Antibody Diluent (S0809; Dako, Agilent) using a polyclonal rabbit anti-mouse p57 antibody (PA5-24428; Thermo Fisher Scientific, Waltham, MA) and a guinea pig anti-mouse synaptopodin antibody (163004; Synaptic Systems, Gottingen, Germany). Subsequently, sections were incubated with secondary antibody using a polyclonal donkey anti-rabbit Alexa Fluor 555 (A31572; Life Technologies, Thermo Fisher Scientific) and a polyclonal goat anti-guinea pig Alexa Flour 488 (A11073; Life Technologies) and Hoechst (H3570; Thermo Fisher Scientific). For immunohistochemical staining of the IL-9R, 5-µm cryosections were air-dried and fixed with 2% paraformaldehyde (EMScience, Thermo Fisher Scientific) for 10 minutes at RT. Unspecific binding was blocked by incubation in 5% horse serum (Vector) in 0.05% Triton X-100 (Sigma Aldrich, St. Louis, MO) and PBS for 30 minutes at RT. Primary antibodies (rat anti-IL9R 1:200; ACRIS Pharmaceuticals, Chapel Hill, NC; and guinea-pig anti-nephrin 1:300; OriGene Technologies, Rockville, MD) were diluted in blocking buffer and allowed to bind over night at 4 °C. Following 3 washes in PBS, secondary antibodies (dye light donkey anti-rat and Cy5-anti guinea-pig, all 1:400; Jackson ImmunoResearch Laboratories, West Grove, PA) diluted in blocking buffer were applied for 30 minutes at RT. Stainings were mounted in Fluoromount (Thermo Fisher Scientific) following 3 washes in PBS and DNA counterstaining with Hoechst (1:1000, 5 minutes at RT; Molecular Probes, Thermo Fisher Scientific) and rhodamine wheat germ agglutinin (1:400; Vector) counterstain. Unspecific IL-9R antibody binding and potential minimal cross-reaction of the affinity purified anti-rat secondary antibody were controlled for by omitting primary rat anti-IL9R antibody and by using kidney sections from $Il9r^{-/-}$ mice. Podocytes and IL-9R localization were visualized in glomeruli using the LSM800 with Airyscan, equipped with 405-, 488-, 561-, and 640-nm lasers, and the ZENblue software (all ZEISS). Total podocyte number per glomerulum was assessed using model-based stereology based on the Weibel and Gomez method[49] validated by White and Bilous[50] in the kidney using the ImageJ software (National Institutes of Health, Bethesda, MD). Electron microscopy was performed using an electron microscope (EM 109; ZEISS) equipped with digital electron microscope cameras (Tröndle, Moorenweis, Germany) and numbers of foot processes per micrometer glomerular basement membrane were determined.

Cell isolation

For isolation of renal leukocytes, mouse kidneys were cut into small pieces and digested in complete medium (Roswell Park Memorial Institute 1640, 10% fetal bovine serum, 1% *N*-2-hydroxyethylpiperazine-*N*′-2-ethanesulfonic acid (HEPES), 1% penicillin/streptomycin; all Gibco, Thermo Fisher Scientific) with collagenase D (0.4 mg/ml; Roche, Basel, Switzerland) and DNase I (100 µg/ml, Roche) for 45 minutes while rotating on a MACSmix tube rotator (Miltenyi, Bergisch Gladbach, Germany) and then further dispersed by using gentleMACS dissociator (Miltenyi). Further leukocyte purification was achieved by Percoll gradient centrifugation (37.5%) (GE Healthcare, Chicago, IL). For isolation of splenocytes, the tissue was meshed through a 70-µm nylon filter and washed with PBS. For analysis of peripheral blood mononuclear cells, 100 to 150 µl ethylenediamine tetraacetic acid blood was collected per mouse. After subsequent erythrocyte lysis with ammonium chloride, cell suspensions were filtered through a 50-µm strainer and used for further analyses. The cell isolation from renal lymph nodes was achieved by meshing the tissue through a 50-µm nylon filter and further washing with PBS. The resulting cell pellet was used for further analysis without additional steps.

Flow cytometry

Nonspecific staining was prevented by incubation with 10% normal mouse serum (Jackson ImmunoResearch). To characterize leukocyte subsets, cell suspensions of mouse kidneys were stained with fluorochrome-coupled antibodies against CD45 (30-F11), Thy1.2 (CD90.2; 30-H12), CD3 (145-2C11), CD4 (RM4-5), CD8 (53-6.7), CD11b (M1/70), TCR-γδ (H57-597 or GL3), Ly6G (1A8), SiglecF (E50-2440), F4/80 (BM8) and a combination of lineage markers, including CD3, CD4, CD8, CD11b, CD11c, CD19 (6D5), CD49b (HMa2), TCR-β (H57-597), TCR-γδ (GL3), GR-1 (RB6-8C5), and Ter119 (Ter119). Phenotyping of Tregs was performed using the

surface markers GITR (YGITR 765), programmed cell death protein 1 (J43), and ICOS (C398.4A). Intranuclear staining, using antibodies against GATA-binding factor 3 (GATA-3) (L50-823), and forkhead box P3 (FJK-16s) was performed with the Transcription Factor Staining Buffer Set (eBioscience, San Diego, CA) according to the manufacturer`s instructions. All antibodies were obtained from BioLegend (San Diego, CA), BD Biosciences (Franklin Lakes, NJ) or eBioscience. Dead cell staining was performed using LIVE/DEAD Fixable Near-IR Dead Stain Kit (Invitrogen, Thermo Fisher Scientific) or Zombie Dye (BioLegend). Absolute numbers of $CD45^+$ cells in kidney cell suspension were determined by staining with fluorochrome-coupled anti-CD45 combined with cell count beads (Countbright; Invitrogen). All samples were acquired on a LSRII flow cytometer (BD Biosciences) and analyzed with the FlowJo software. For leukocyte analyses, events were first gated for singlets according to forward scatter (area vs. height) properties, followed by gating for the pan-leukocyte marker $CD45^+$ and live cells (exclusion of dead cells stained as we have already detailed). Leukocytes subsets were gated according to the appropriate marker combination as detailed in the respective figures.

Isolation of glomeruli and tubules

The isolation of glomeruli from the murine kidney was performed as described beforehand.[51] Briefly, mice were perfused with Dynabeads (Thermo Fischer Scientific) and after extraction of the kidney, the inner and outer medulla were removed and discarded. Subsequently, kidneys were digested with collagenase I for 20 minutes at 37 °C and the glomeruli, containing the magnetic beads, were separated from the renal tubules by magnetic separation using the DynaMag-2 magnet (Invitrogen).

Cell culture

Undifferentiated murine podocytes (a kind gift from P. Mundel, Boston, MA) were maintained under permissive conditions (32 °C, 5% CO_2, Roswell Park Memorial Institute 1640 supplemented with 10% fetal calf serum, 10 mmol/l HEPES, 1 mmol/l sodium pyruvate, 100 U/ml penicillin, 100 mg/ml streptomycin (all Gibco) and 10 U/ml interferon-γ (PeproTech, London, UK). For differentiation, podocytes were cultured for 12 days in nonpermissive conditions (37 °C, 7,4% CO_2, Roswell Park Memorial Institute 1640 supplemented with 10% fetal calf serum, 10 mmol/l HEPES, 1 mmol/l sodium pyruvate, 100 U/ml penicillin, 100 mg/ml streptomycin) and then used for the experiments. Podocytes were treated with IL-9 (10, 50, 100, or 300 mg/ml; R&D Systems, Bio-Techne, Minneapolis, MN) for 24 hours followed by coincubation with Adriamycin (0.5 μg/ml) for 16 hours. Podocyte apoptosis was quantified by flow cytometry using annexin V (fluorescein isothiocyanate) fluorescence staining (BioLegend).

In vitro cultivation of T cells

Leukocytes from the kidneys and spleen of $Il9^{Cre}R26R^{tdtomato}$ mice were isolated and naïve ($CD3^+CD4^+CD62L^+CD44^{low}$) and effector T cells ($CD3^+CD4^+CD62L^-CD44^{high}$) were purified by flow cytometry. T cells were cultured in Iscove's modified Dulbecco medium (Gibco) supplemented with 5% fetal calf serum, 50 U/ml penicillin, 50 μg/ml streptomycin, 1% HEPES and 50 μmol/l β-mercaptoethanol. For Th9 cell conditions, cells were cultured in the presence of 10 ng/ml IL-2, 25 ng/ml IL-1β, 10 ng/ml IL-6, 5 ng/ml transforming growth factor-β, and 10 ng/ml IL-4 with or without additional TCR stimulation by plate-bound anti-CD3e (1 μg/ml) and anti-CD28 (10 μg/ml). Cells were cultured at 37 °C and 5% CO_2 for 72 hours and analyzed by flow cytometry after staining with LIVE/DEAD Fixable Near-IR staining kit (Invitrogen).

Real-time PCR analysis

Total RNA of isolated kidney compartments or murine podocytes was prepared according to standard laboratory methods. After reverse transcription to cDNA, real-time PCR was performed for 45 cycles (initial denaturation at 95 °C for 10 minutes, followed by cycles of denaturation at 95 °C for 15 seconds, and primer annealing and elongation at 60 °C for 1 minutes) with 1 μl of cDNA samples in the presence of 0.5 μl of specific murine primers. TaqMan Gene Expression Assays and a StepOnePlus Real-Time PCR system (both Thermo Fisher Scientific) were used for quantification of the housekeeping gene (*Hprt1*) and the genes of interest. All samples were run in duplicates.

Human blood samples

The study was approved by the local ethics committee of the chamber of physicians in Hamburg (approval number PV4806 and PV4780) and it was conducted in accordance with the ethical principles stated by the Declaration of Helsinki. Informed consent was obtained from all participating patients. Serum samples were centrifuged and stored at −20 °C. IL-9 was analyzed using the Meso Scale immunoassay (Meso Scale Diagnostics, Rockville, MD), following the manufacturer`s protocol.

Statistics

Statistical comparisons were performed with the Prism software (GraphPad Software, San Diego, CA), using the Mann-Whitney test. In case of ≥3 groups, 1-way analysis of variance was used followed by a *post hoc* analysis with Newman-Keuls test for multiple comparisons. A P value of <0.05 was considered to be statistically significant.

DISCLOSURE

All the authors declared no competing interests.

ACKNOWLEDGMENTS

J-ET is supported by the Collaborative Research Center 1192 (grant TP A6) and Emmy Noether grant TU 316/1-2 of the Deutsche Forschungsgemeinschaft. TX (grant TP A6), MA (grant TP A6), A-CG (grant TP A6), MW (grant TP A6), CR (grant TP A6), CM-S (grant TP B3), TW (grant TP C1, B6), TF (grant TP A7), EH (grant TP C1, B1), TBH (grant TP C1), and UP (grant TP A1) are supported by the Collaborative Research Center 1192. HT is supported by Emmy Noether grant TA 1154/1-1 of the Deutsche Forschungsgemeinschaft. JSzW is supported by the Collaborative Research Centers SFB841 (grant TP A6) and SFB1328 (grant TP A12).

Patient sera were provided by the Hamburg Glomerulonephritis Registry. We thank all patients and nephrologists who participate in the Hamburg Glomerulonephritis Registry. We also thank Andrew McKenzie (Cambridge, UK), Brigitta Stockinger (London, UK), and Jean-Christophe Renauld (Brussels, Belgium) for providing $Il9^{-/-}$ mice, $Il9^{Cre}$ mice, and $Il9r^{-/-}$ mice, respectively, as well as Ella Weinert and Christina Bossman for excellent technical assistance.

SUPPLEMENTARY MATERIAL

Supplementary File (PDF)

Figure S1. Cellular immune response is unaltered in the kidneys of WT and $Il9^{-/-}$ mice with AN. (**A**) Representative flow cytometry plots of renal leukocyte subsets isolated from naïve WT mice, as well as

from WT and *Il9*$^{-/-}$ mice at day 14 of AN. Gating strategy is specified in brackets and numbers indicate the percentage of cells in the gates or quadrants. (**B**) Quantification of absolute numbers of CD45^{+} cells and T cell and myeloid cell subsets in the kidney in the respective groups (naïve WT controls, $n = 6$; WT AN day 14, $n = 14$; *Il9*$^{-/-}$ AN day 14, $n = 14$). (**B**) Bars represent mean ± SEM. Open and filled circles represent individual animals. Data are pooled from 2 individual experiments with similar results. MNP = mononuclear phagocytes.

Figure S2. Phenotype of Tregs in renal lymph nodes and kidneys of WT and *Il9*$^{-/-}$ mice. Representative flow cytometry plots and quantification of surface expression markers on Tregs isolated from (**A**) renal lymph nodes and (**B**) kidneys of naïve WT and *Il9*$^{-/-}$ mice, as well as from WT and *Il9*$^{-/-}$ mice at day 14 of AN (naïve WT, $n = 6$; naïve *Il9*$^{-/-}$, $n = 7$; WT AN day 14, $n = 16$; *Il9*$^{-/-}$ AN day 14, $n = 14$). Gating strategy is specified in brackets and (**A,B**) bars represent mean ± SEM. Open and filled circles represent individual animals. Data are pooled from 2 individual experiments with similar results. As baseline mean fluorescence intensity (MFI) of the markers in naïve WT mice differed between the 2 experiments, for better comparison, MFI was normalized to the naïve WT level.

Figure S3. Phenotype of *Il9*$^{-/-}$ mice in nephrotoxic nephritis (NTN). (**A**) Representative photographs of periodic acid–Schiff–stained kidney sections (original magnification ×400; bars = 50 μm), (**B**) histopathological quantification of glomerular and interstitial damage and analysis of (**C**) albuminuria and (**D**) blood urea nitrogen, as a renal function parameter, in naïve WT mice, as well as WT and *Il9*$^{-/-}$ mice at day 11 after induction of NTN (naïve WT controls, $n = 6$; WT NTN day 11, $n = 10$; *Il9*$^{-/-}$ NTN day 11, $n = 10$). (**B–D**) Bars represent mean ± SEM. Open and filled circles represent individual animals. Data are pooled from 2 individual experiments with similar results. *$P < 0.05$.

Figure S4. Analysis of IL-9 fate-mapping signal in nonlymphoid renal leukocytes, in peripheral blood cells and in the spleen. (**A**) Representative flow cytometric analyses and quantification of renal cells isolated from naïve *Il9*^{Cre}*R26r*^{tdtomato} fate reporter mice and *Il9*^{Cre}*R26r*^{tdtomato} mice at day 14 of AN (naïve, $n = 5$; AN day 14, $n = 6$). (**B,C**) Representative flow cytometric analysis and quantification of IL-9^{fm+} cells in (**B**) peripheral blood mononuclear cells (PBMCs) and (**C**) the spleen (naïve, $n = 5$; AN day 14, $n = 6$). Data are pooled from 2 independent experiments with similar results. Gating strategy is specified in brackets and numbers indicate the percentage of cells in the gates. (**A–C**) Bars represent mean ± SEM. Open and filled circles represent individual animals.

Figure S5. Induction of IL-9 production in T cells from the spleen and kidney. Representative flow cytometry plots and quantification of IL-9 fate-mapping signal (IL-9^{fm}) in (**A**) CD62L^{+}CD44^{low} naïve CD4^{+} T cells isolated from the spleen and (**B**) CD62L^{-}CD44^{high} effector CD4^{+} T cells isolated from the kidneys of *Il9*^{Cre}*R26r*^{tdtomato} fate reporter mice by flow cytometric cell sorting. Purified T cells were cultured for 72 hours with either IL-2 alone (Th0), or IL-2, IL-6, IL-4, IL-1β, and TGF-β (Th9), or Th9 conditions with additional T cell receptor (TCR) stimulation by anti-CD3e and anti-CD28. (**C**) mRNA expression analysis of renal cortex from naïve WT mice and from WT mice at day 14 after induction of AN (naïve, $n = 3$; AN day 14, $n = 12–13$). Bars in (**A**) to (**C**) represent mean ± SEM and circles represent individual animals. (**A–C**) Data are pooled from 2 individual experiments.

Table S1. Characteristics of primary FSGS patients and healthy controls. Characteristics of (**A**) patients with primary FSGS and (**B**) healthy controls and (**C**) statistical comparison of characteristics between the 2 groups. Values are expressed as *n* (%), or mean ± SEM. n.a. = not available.

REFERENCES

1. Gansevoort RT, Correa-Rotter R, Hemmelgarn BR, et al. Chronic kidney disease and cardiovascular risk: epidemiology, mechanisms, and prevention. *Lancet*. 2013;382:339–352.
2. Kurts C, Panzer U, Anders HJ, Rees AJ. The immune system and kidney disease: basic concepts and clinical implications. *Nat Rev Immunol*. 2013;13:738–753.
3. Turner JE, Becker M, Mittrucker HW, Panzer U. Tissue-resident lymphocytes in the kidney. *J Am Soc Nephrol*. 2018;29:389–399.
4. Deng Y, Wang Z, Chang C, et al. Th9 cells and IL-9 in autoimmune disorders: Pathogenesis and therapeutic potentials. *Hum Immunol*. 2017;78:120–128.
5. Gessner A, Blum H, Rollinghoff M. Differential regulation of IL-9-expression after infection with Leishmania major in susceptible and resistant mice. *Immunobiology*. 1993;189:419–435.
6. Nowak EC, Weaver CT, Turner H, et al. IL-9 as a mediator of Th17-driven inflammatory disease. *J Exp Med*. 2009;206:1653–1660.
7. Eller K, Wolf D, Huber JM, et al. IL-9 production by regulatory T cells recruits mast cells that are essential for regulatory T cell-induced immune suppression. *J Immunol*. 2011;186:83–91.
8. Lu LF, Lind EF, Gondek DC, et al. Mast cells are essential intermediaries in regulatory T-cell tolerance. *Nature*. 2006;442:997–1002.
9. Veldhoen M, Uyttenhove C, van Snick J, et al. Transforming growth factor-beta 'reprograms' the differentiation of T helper 2 cells and promotes an interleukin 9-producing subset. *Nat Immunol*. 2008;9:1341–1346.
10. Dardalhon V, Awasthi A, Kwon H, et al. IL-4 inhibits TGF-beta-induced Foxp3+ T cells and, together with TGF-beta, generates IL-9+ IL-10+ Foxp3(-) effector T cells. *Nat Immunol*. 2008;9:1347–1355.
11. Wilhelm C, Turner JE, Van Snick J, et al. The many lives of IL-9: a question of survival? *Nat Immunol*. 2012;13:637–641.
12. Wilhelm C, Hirota K, Stieglitz B, et al. An IL-9 fate reporter demonstrates the induction of an innate IL-9 response in lung inflammation. *Nat Immunol*. 2011;12:1071–1077.
13. Turner JE, Morrison PJ, Wilhelm C, et al. IL-9-mediated survival of type 2 innate lymphoid cells promotes damage control in helminth-induced lung inflammation. *J Exp Med*. 2013;210:2951–2965.
14. Stassen M, Arnold M, Hultner L, et al. Murine bone marrow-derived mast cells as potent producers of IL-9: costimulatory function of IL-10 and kit ligand in the presence of IL-1. *J Immunol*. 2000;164:5549–5555.
15. Hultner L, Druez C, Moeller J, et al. Mast cell growth-enhancing activity (MEA) is structurally related and functionally identical to the novel mouse T cell growth factor P40/TCGFIII (interleukin 9). *Eur J Immunol*. 1990;20:1413–1416.
16. Uyttenhove C, Simpson RJ, Van Snick J. Functional and structural characterization of P40, a mouse glycoprotein with T-cell growth factor activity. *Proc Natl Acad Sci U S A*. 1988;85:6934–6938.
17. Dugas B, Renauld JC, Pene J, et al. Interleukin-9 potentiates the interleukin-4-induced immunoglobulin (IgG, IgM and IgE) production by normal human B lymphocytes. *Eur J Immunol*. 1993;23:1687–1692.
18. Vink A, Warnier G, Brombacher F, Renauld JC. Interleukin 9-induced in vivo expansion of the B-1 lymphocyte population. *J Exp Med*. 1999;189:1413–1423.
19. Fontaine RH, Cases O, Lelievre V, et al. IL-9/IL-9 receptor signaling selectively protects cortical neurons against developmental apoptosis. *Cell Death Differ*. 2008;15:1542–1552.
20. Gerlach K, Hwang Y, Nikolaev A, et al. TH9 cells that express the transcription factor PU.1 drive T cell-mediated colitis via IL-9 receptor signaling in intestinal epithelial cells. *Nat Immunol*. 2014;15:676–686.
21. Dong Q, Louahed J, Vink A, et al. IL-9 induces chemokine expression in lung epithelial cells and baseline airway eosinophilia in transgenic mice. *Eur J Immunol*. 1999;29:2130–2139.
22. Rauber S, Luber M, Weber S, et al. Resolution of inflammation by interleukin-9-producing type 2 innate lymphoid cells. *Nat Med*. 2017;23:938–944.
23. Zhang W, Tang T, Nie D, et al. IL-9 aggravates the development of atherosclerosis in ApoE$^{-/-}$ mice. *Cardiovasc Res*. 2015;106:453–464.
24. Li Q, Ming T, Wang Y, et al. Increased Th9 cells and IL-9 levels accelerate disease progression in experimental atherosclerosis. *Am J Transl Res*. 2017;9:1335–1343.
25. Zhang L, Wu JH, Otto JC, et al. Interleukin-9 mediates chronic kidney disease-dependent vein graft disease: a role for mast cells. *Cardiovasc Res*. 2017;113:1551–1559.
26. Kortekaas KA, de Vries DK, Reinders ME, et al. Interleukin-9 release from human kidney grafts and its potential protective role in renal ischemia/reperfusion injury. *Inflamm Res*. 2013;62:53–59.
27. de Lira Silva NS, Borges BC, da Silva AA, et al. The deleterious impact of interleukin 9 to hepatorenal physiology. *Inflammation*. 2019;42:1360–1369.

28. Wang Y, Wang YP, Tay YC, Harris DC. Progressive Adriamycin nephropathy in mice: sequence of histologic and immunohistochemical events. *Kidney Int*. 2000;58:1797–1804.
29. Sato Y, Yanagita M. Immune cells and inflammation in AKI to CKD progression. *Am J Physiol Renal Physiol*. 2018;315:F1501–F1512.
30. Singhera GK, MacRedmond R, Dorscheid DR. Interleukin-9 and -13 inhibit spontaneous and corticosteroid induced apoptosis of normal airway epithelial cells. *Exp Lung Res*. 2008;34:579–598.
31. Fogo AB. Causes and pathogenesis of focal segmental glomerulosclerosis. *Nat Rev Nephrol*. 2015;11:76–87.
32. Cao Q, Wang C, Zheng D, et al. IL-25 induces M2 macrophages and reduces renal injury in proteinuric kidney disease. *J Am Soc Nephrol*. 2011;22:1229–1239.
33. Lu J, Cao Q, Zheng D, et al. Discrete functions of M2a and M2c macrophage subsets determine their relative efficacy in treating chronic kidney disease. *Kidney Int*. 2013;84:745–755.
34. Duster M, Becker M, Gnirck AC, et al. T cell-derived IFN-gamma downregulates protective group 2 innate lymphoid cells in murine lupus erythematosus. *Eur J Immunol*. 2018;48:1364–1375.
35. Riedel JH, Becker M, Kopp K, et al. IL-33-mediated expansion of type 2 innate lymphoid cells protects from progressive glomerulosclerosis. *J Am Soc Nephrol*. 2017;28:2068–2080.
36. Wynn TA. Type 2 cytokines: mechanisms and therapeutic strategies. *Nat Rev Immunol*. 2015;15:271–282.
37. Gieseck RL 3rd, Wilson MS, Wynn TA. Type 2 immunity in tissue repair and fibrosis. *Nat Rev Immunol*. 2018;18:62–76.
38. Allen JE, Sutherland TE. Host protective roles of type 2 immunity: parasite killing and tissue repair, flip sides of the same coin. *Semin Immunol*. 2014;26:329–340.
39. Elyaman W, Bradshaw EM, Uyttenhove C, et al. IL-9 induces differentiation of TH17 cells and enhances function of FoxP3+ natural regulatory T cells. *Proc Natl Acad Sci U S A*. 2009;106:12885–12890.
40. Li H, Nourbakhsh B, Ciric B, et al. Neutralization of IL-9 ameliorates experimental autoimmune encephalomyelitis by decreasing the effector T cell population. *J Immunol*. 2010;185:4095–4100.
41. Temann UA, Ray P, Flavell RA. Pulmonary overexpression of IL-9 induces Th2 cytokine expression, leading to immune pathology. *J Clin Invest*. 2002;109:29–39.
42. Sun YB, Qu X, Zhang X, et al. Glomerular endothelial cell injury and damage precedes that of podocytes in adriamycin-induced nephropathy. *PLoS One*. 2013;8:e55027.
43. Stangou M, Papagianni A, Bantis C, et al. Detection of multiple cytokines in the urine of patients with focal necrotising glomerulonephritis may predict short and long term outcome of renal function. *Cytokine*. 2012;57:120–126.
44. Townsend JM, Fallon GP, Matthews JD, et al. IL-9-deficient mice establish fundamental roles for IL-9 in pulmonary mastocytosis and goblet cell hyperplasia but not T cell development. *Immunity*. 2000;13:573–583.
45. Shinkai Y, Rathbun G, Lam KP, et al. RAG-2-deficient mice lack mature lymphocytes owing to inability to initiate V(D)J rearrangement. *Cell*. 1992;68:855–867.
46. Steenwinckel V, Louahed J, Orabona C, et al. IL-13 mediates in vivo IL-9 activities on lung epithelial cells but not on hematopoietic cells. *J Immunol*. 2007;178:3244–3251.
47. Panzer U, Steinmetz OM, Paust HJ, et al. Chemokine receptor CXCR3 mediates T cell recruitment and tissue injury in nephrotoxic nephritis in mice. *J Am Soc Nephrol*. 2007;18:2071–2084.
48. Liu F, Song Y, Liu D. Hydrodynamics-based transfection in animals by systemic administration of plasmid DNA. *Gene Ther*. 1999;6:1258–1266.
49. Weibel ER, Gomez DM. A principle for counting tissue structures on random sections. *J Appl Physiol*. 1962;17:343–348.
50. White KE, Bilous RW. Estimation of podocyte number: a comparison of methods. *Kidney Int*. 2004;66:663–667.
51. Takemoto M, Asker N, Gerhardt H, et al. A new method for large scale isolation of kidney glomeruli from mice. *Am J Pathol*. 2002;161:799–805.

Supplementary Figure 1

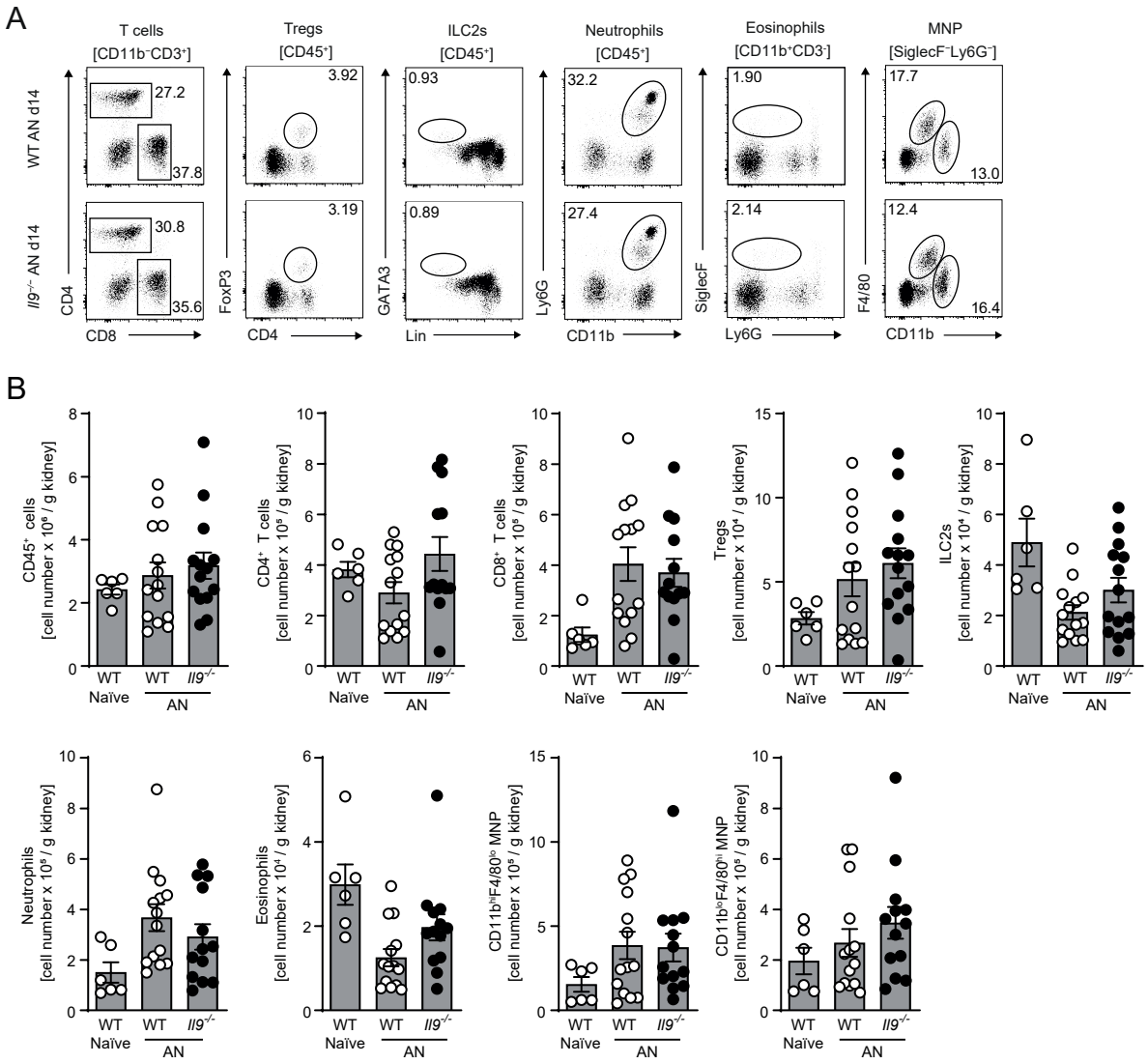

Supplementary Figure 1: Cellular immune response is unaltered in the kidneys of WT and *Il9*$^{-/-}$ mice with AN.

(A) Representative flow cytometry plots of renal leukocyte subsets isolated from naïve WT mice, as well as from WT and *Il9*$^{-/-}$ mice at day 14 of AN. Gating strategy is specified in brackets and numbers indicate the percentage of cells in the gates or quadrants. **(B)** Quantification of absolute numbers of CD45^{+} cells, T cell and myeloid cell subsets in the kidney in the respective groups (naïve WT controls *n*=6, WT AN d14 *n*=14, *Il9*$^{-/-}$ AN d14 *n*=14). Bars in B represent mean ± SEM. Open and filled circles represent individual animals. Data are pooled from two individual experiments with similar results. MNP = mononuclear phagocytes.

Supplementary Figure 2

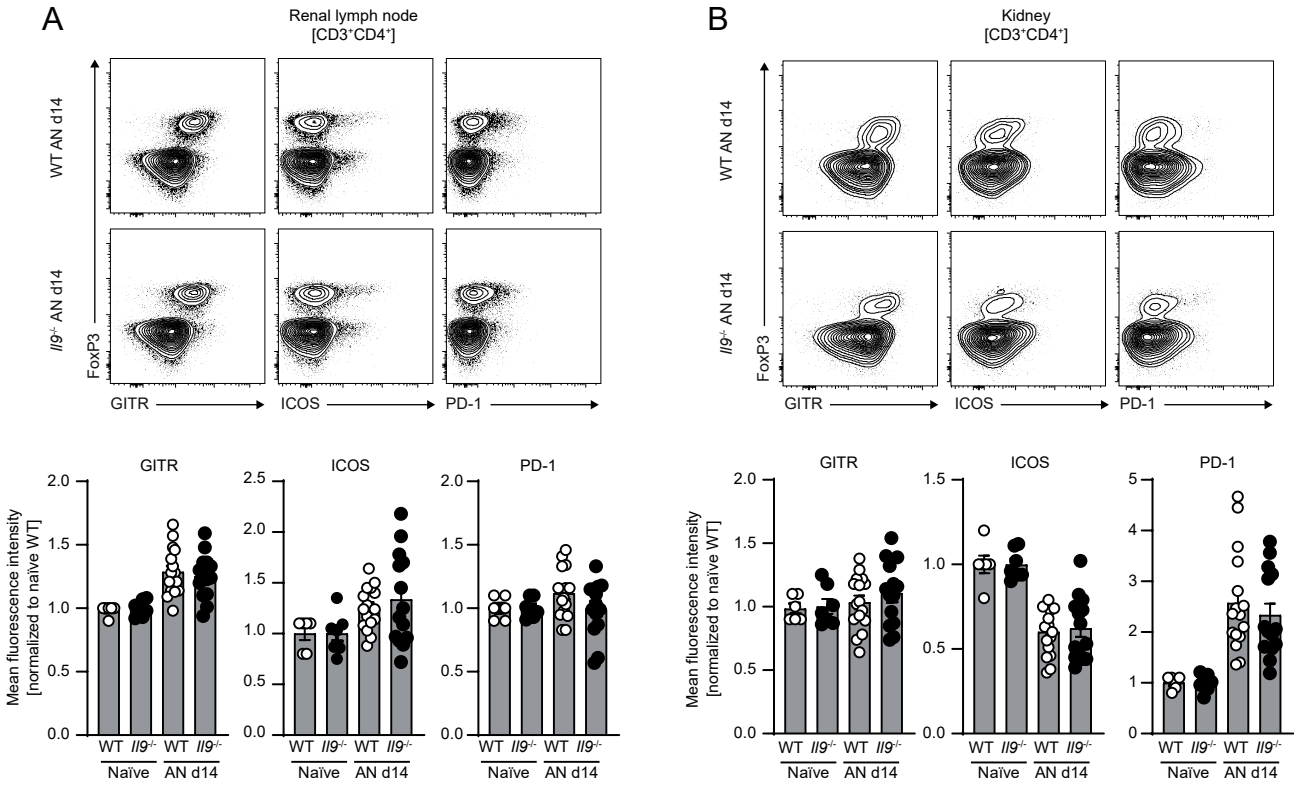

Supplementary Figure 2: Phenotype of Tregs in renal lymph nodes and kidneys of WT and *Il9*$^{-/-}$ mice.

Representative flow cytometry plots and quantification of surface expression markers on Tregs isolated from renal lymph nodes **(A)** and kidneys **(B)** of naïve WT and *Il9*$^{-/-}$ mice, as well as from WT and *Il9*$^{-/-}$ mice at day 14 of AN (naïve WT *n*=6, naïve *Il9*$^{-/-}$ *n*=7, WT AN d14 *n*=16, *Il9*$^{-/-}$AN d14 *n*=14). Gating strategy is specified in brackets and bars in A and B represent mean ± SEM. Open and filled circles represent individual animals. Data are pooled from two individual experiments with similar results. As baseline mean fluorescence intensity (MFI) of the markers in naïve WT mice differed between the two experiments, for better comparison, MFI was normalized to the naïve WT level.

Supplementary Figure 3

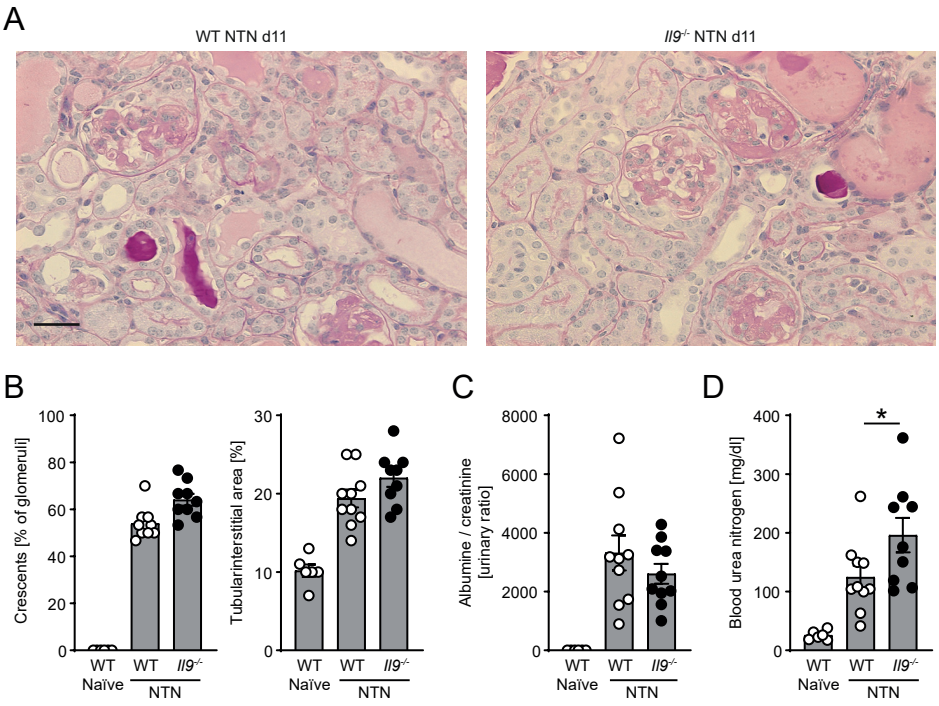

Supplementary Figure 3: Phenotype of *Il9*$^{-/-}$ mice in nephrotoxic nephritis.

(A) Representative photographs of periodic acid-Schiff-stained kidney sections (original magnification 400x, scale bars represent 50 µm), **(B)** histopathological quantification of glomerular and interstitial damage and analysis of **(C)** albuminuria and **(D)** blood urea nitrogen, as a renal function parameter, in naïve WT mice, as well as WT and *Il9*$^{-/-}$ mice at day 11 after induction of nephrotoxic nephritis (NTN) (naïve WT controls n=6, WT NTN d11 n=10, *Il9*$^{-/-}$ NTN d11 n=10). Bars in B-D represent mean ± SEM. Open and filled circles represent individual animals. Data are pooled from two individual experiments with similar results. (* P<0.05).

Supplementary Figure 4

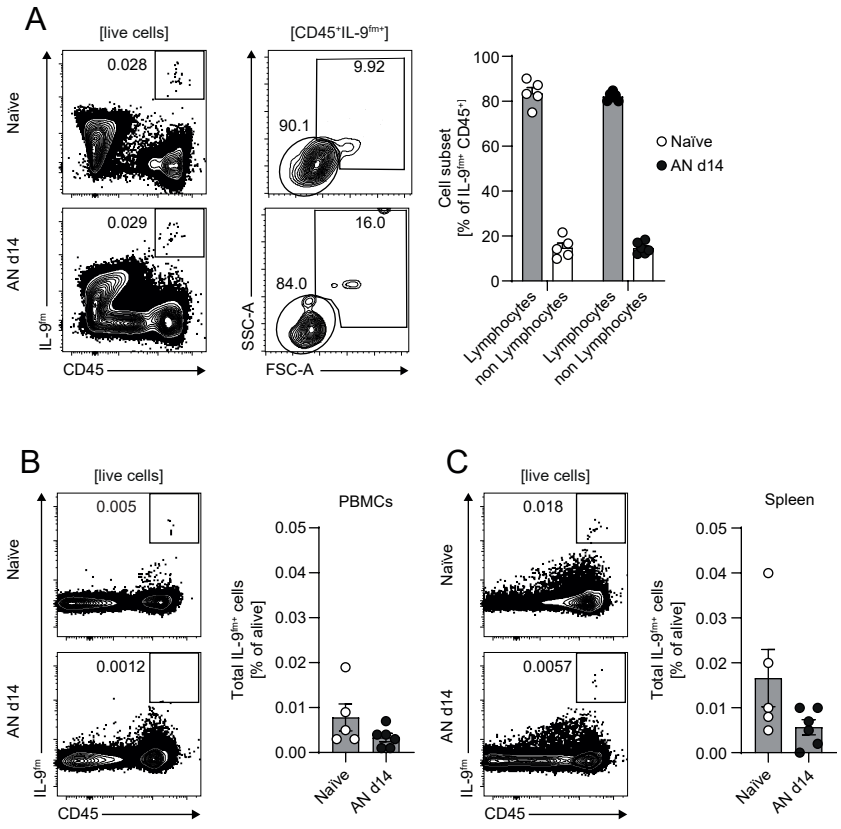

Supplementary Figure 4: Analysis of IL-9 „fate-mapping“ signal in non-lymphoid renal leukocytes, in peripheral blood cells and in the spleen.

(A) Representative flow cytometric analyses and quantification of renal cells isolated from naïve *Il9*^{Cre}*R26r*^{tdtomato} “fate reporter” mice and *Il9*^{Cre}*R26r*^{tdtomato} mice at day 14 of AN (naïve *n*=5, AN d14 *n*=6). **(B, C)** Representative flow cytometric analysis and quantification of IL-9^{fm+} cells in **(B)** peripheral blood mononuclear cells (PBMCs) and **(C)** the spleen (naïve *n*=5, AN d14 *n*=6). Data are pooled from two independent experiments with similar results. Gating strategy is specified in brackets and numbers indicate the percentage of cells in the gates. Bars in A-C represent mean ± SEM. Open and filled circles represent individual animals.

Supplementary Figure 5

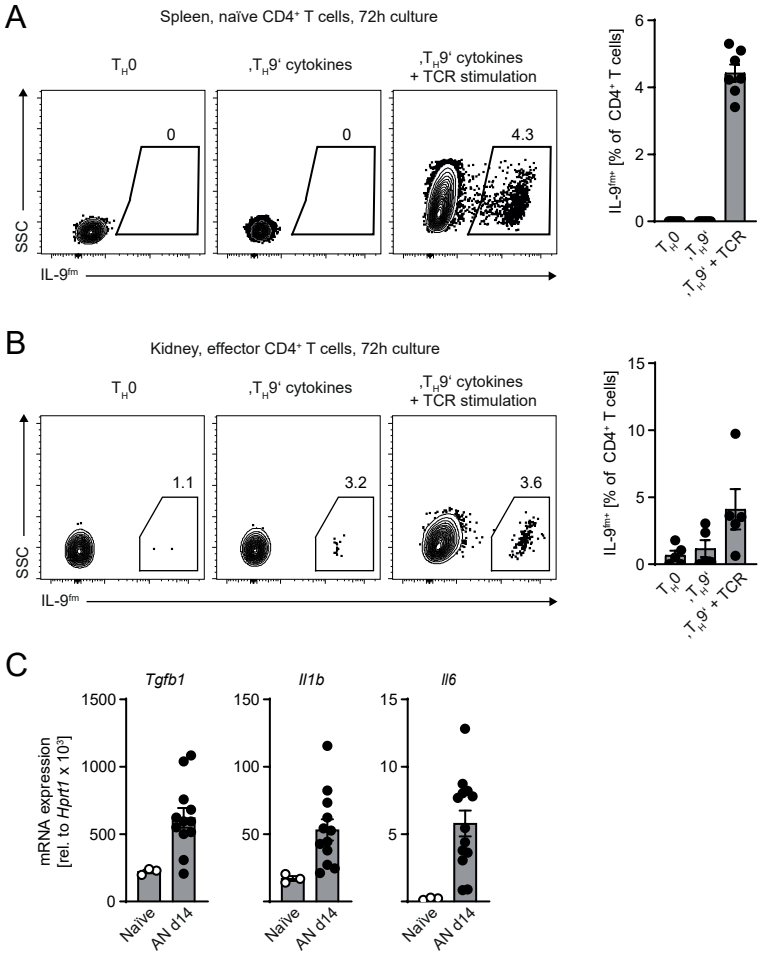

Supplementary Figure 5: Induction of IL-9 production in T cells from the spleen and kidney.

Representative flow cytometry plots and quantification of IL-9 „fate-mapping" signal (IL-9^{fm}) in **(A)** CD62L^{+}CD44^{low} naïve CD4^{+} T cells isolated from the spleen and **(B)** CD62L^{-}CD44^{high} effector CD4^{+} T cells isolated from the kidneys of *Il9*^{Cre}*R26r*^{tdtomato} "fate reporter" mice by flow cytometric cell sorting. Purified T cells were cultured for 72h with either IL-2 alone ('T_H0'), or IL-2, IL-6, IL-4, IL-1β and TGF-β ('T_H9'), or 'T_H9' conditions with additional T cell receptor (TCR) stimulation by anti-CD3e and anti-CD28. **(C)** mRNA expression analysis of renal cortex from naïve WT mice and from WT mice at day 14 after induction of AN (naïve *n*=3, AN d14 *n*=12-13). Bars in A-C represent mean ± SEM and circles represent individual animals. Data in A-C are pooled from two individual experiments.

Supplementary Table 1

A

Sex	Age (years)	Creatinine (mg/dL)	Proteinuria (mg/24h)	Immunosuppression at time of sample	History of immunosuppression	IL-9 level (pg/mL)
m	43	1.1	4873	none	Prednisolone, Cyclophosphamide	1.31
m	51	3.0	6389	none	none	3.93
m	34	1.3	12537	none	Prednisolone	1.33
m	64	5.9	9222	Prednisolone	Prednisolone	1.33
m	56	n.a.	n.a.	Prednisolone, Cyclosporin A	Prednisolone, Cyclosporin A	1.32
m	74	1.6	1600	Cyclosporin A	Cyclosporin A	3.01
m	68	n.a.	n.a.	Prednisolone	none	4.31
m	77	2.5	4325	none	Prednisolone	1.8
f	20	0.8	3989	Prednisolone	none	0.7
m	60	0.8	469	Prednisolone	Prednisolone, Cyclophosphamide	0.51
f	73	0.9	n.a.	n.a.	none	2.01
m	39	1.0	598	Prednisolone	Prednisolone	2.52
m	50	3.0	5385	Prednisolone, Cyclosporin A	Prednisolone, Cyclosporin A, Mycophenolate mofetil	2.61
f	68	1.1	4639	none	none	0.39

B

Sex	Age (years)	IL-9 level (pg/mL)
f	36	1.77
m	40	1.16
f	35	1.79
f	40	1.0
m	56	0.42
m	34	0.65
f	64	0.51
m	56	0.74
m	36	2.1
m	42	2.33
m	30	0.56
m	50	0.79
f	36	0.47
f	45	1.01

C

	Controls (n=14)	FSGS (n=14)	P-value
Male	8 (53 %)	11 (78 %)	0.419
Age (years)	43±3	55±4	0.024
IL-9 (pg/mL)	1.09±0.17	1.93±0.32	0.045

Supplementary Table 1: Characteristics of primary FSGS patients and healthy controls

(A) Characteristics of patients with primary FSGS, **(B)** healthy controls and **(C)** statistical comparison of characteristics between the two groups. Values are expressed as n (%), or mean ± SEM. n.a. = not available.

2. Darstellung der Publikation

Einleitung

Chronische Nierenerkrankungen

Chronische Nierenerkrankungen (engl. Chronic Kidney Diseases, CKD) gehen mit einer irreversiblen Abnahme der inkretorischen und exkretorischen Funktion der Niere einher. Eine CKD liegt vor, wenn seit über drei Monaten Auffälligkeiten in der Struktur oder Funktion der Niere vorliegen (z.B. eine GFR von <60 mL/min/1,73m^2). Histologisch fallen die Nieren bei CKDs mit Glomerulosklerose, Entzündung des Tubulointerstitiums und Fibrose auf.

CKDs stellen ein globales Problem dar, 8 bis 16% der weltweiten Population sind betroffen (Chen et al, 2019). Die Hauptursachen stellen insbesondere in der westlichen Bevölkerung Diabetes und arterielle Hypertension dar (Chen et al, 2019). Es liegt eine Assoziation zu kardiovaskulären Erkrankungen und höherer Morbidität und Mortalität vor (Chang et al., 2014, Narres et al., 2016). Bei Fortschreiten der Erkrankung sind meist Nierenersatzverfahren notwendig, welche ebenfalls mit einer erhöhten Mortalität einhergehen.

Die Adriamycin-Nephropathie – ein Mausmodell für die proteinurische CKD

Die Adriamycin-Nephropathie (AN) stellt ein murines Modell der chronischen Nierenerkrankung mit Proteinurie dar (Lee und Harris, 2011). Adriamycin – in Deutschland unter dem Namen Doxorubicin geläufig – ist ein Zytostatikum und wird zu den Anthrazyklinen gezählt. Während es im Menschen hepatisch metabolisiert wird, akkumuliert Adriamycin bei Mäusen in der Niere. Hierdurch wird die vorwiegend nephrotoxische Wirkung bei der Maus im Gegensatz zur hauptsächlich kardiotoxischen im Menschen erklärt. Nach intravenöser Gabe kommt es innerhalb weniger Tage zur Ausbildung eines nephrotischen Syndroms mit Proteinurie und Hypalbuminämie mit folgender Ödembildung. Histopathologisch stellt sich die Niere mit fokaler und segmentaler Glomerulosklerose, tubulointerstitieller Inflammation sowie Fibrosierung des Parenchyms dar (Lee und Harris, 2011). Die glomeruläre Filtrationsbarriere zeigt eine Verschmelzung der Podozytenfußfortsätze sowie die Verschmälerung des Endothels, welche mit einem Verlust der Filterfunktion einhergehen.

Der initiale Schaden wird neben der DNA-Interkalation zurückgeführt auf eine direkte zytotoxische Wirkung des Adriamycins auf die Zellen, indem vermehrt freie Radikale (Barbey et al., 1989) sowie reaktive Sauerstoffspezies freigesetzt werden. Zusätzlich wird der RAGE-Rezeptor (eng. *receptor of advanced glycation end products*) durch Hochregulation seiner

Liganden aktiviert, welches ein inflammatorisches Milieu schafft und profibrotische Wachstumsfaktoren wie z.B. TGF-β freisetzt (Guo et al., 2008).

Im Rahmen der inflammatorischen Reaktion auf den Gewebeschaden kommt es zu einer Infiltration von insbesondere Lymphozyten in die Niere (Wang et al., 2000). Diese haben unterschiedliche Auswirkungen auf den Verlauf der AN; so führt die Depletion von $CD4^+$-T-Zellen zu einem aggravierten Verlauf (Wang et al., 2001). Die zugrundeliegenden Mechanismen sind noch weitestgehend unklar.

Das Zytokin IL-9

IL-9 zählt zusammen mit IL-2, IL-4, IL-7, IL-15 und IL-21 zu den Zytokinen, die an Rezeptoren mit einer gemeinsamen *common γ-chain* binden. Die *α-chain* ist stets ligandenspezifisch. Im Menschen findet sich das IL-9-Gen auf Chromosom 5, wo es in der Nähe der typischen T_H2-Zytokine IL-4, IL-5 und IL-13 lokalisiert ist, während es bei der Maus auf Chromosom 13 liegt. (Mock et al, 1990). Initial wurde es als Wachstumsfaktor für T- und Mastzellen beschrieben (Uyttenhove et al., 1988; Hultner et al., 1990).

Quellen von IL-9

IL-9 wird sowohl von myeloischen als auch lymphoiden Zellen produziert. Die Produktion findet u.a. in T-Lymphozyten, insbesondere den T_H2-Zellen, aber auch T_H17-Zellen und T_{regs}, sowie Mastzellen statt (Goswami und Kaplan, 2011).

In vitro konnten durch Stimulation mit TGF-β und IL-4 naive T-Zellen zu sog. „Th-9"-Zellen polarisiert werden (Veldhoen et al., 2008). Diese zeigen eine Hochregulation der Transkriptionsfaktoren PU.1 und IRF4 und produzieren in hohem Maße IL-9. Auch wenn in der Literatur diese Zellen immer wieder als eigenständige Subpopulation der $CD4^+$-Zellen diskutiert werden, zeigen *in vivo* Nachweise, dass diese Zellen nur transient IL-9 produzieren. Jäger et al. (2009) wiesen z.B. nach, dass *in vitro* differenzierte und in die Maus transferierte Th-9-Zellen dazu fähig sind, die sog. experimentelle Autoimmunenzephalomyelitis (EAE) auszulösen, welches ein Tiermodell der multiplen Sklerose darstellt. Diese Zellen produzierten jedoch nach Isolation *ex vivo* jedoch hauptsächlich IFN-γ und IL-4 und waren somit instabil (Burkett et al., 2014). Vor diesem Hintergrund wird die Möglichkeit transienter ‚Th-9'-Zellen im Rahmen der T-Zell-Plastizität *in vivo* diskutiert.

Durch den Einsatz sog. ‚fate-reporter'-Mäusen, in denen IL-9-exprimierende Zellen *in vivo* markiert werden können, wurden Innate Lymphoid Cells (ILCs) als Hauptproduzent von IL-9 in der Lungen-Inflammation identifiziert (Wilhelm et al., 2012). ILCs (engl. *innate lymphoid*

cells = angeborene lymphoide Zellen) exprimieren keinen Antigenrezeptor, schütten jedoch ähnliche Entzündungsmediatoren wie die T-Lymphozyten aus. Typ-2-ILCs (ILC2s) werden durch IL-2 aus T-Zellen und IL-33 aktiviert und können IL-9 produzieren.

Zielzellen des IL-9-Signalwegs

Neben der Funktion als Wachstumsfaktor von T- und Mastzellen exprimieren ILC2s auch selbst den IL-9-Rezeptor (Wilhelm et al., 2012): In einem Mausmodell der Wurminfektion war das IL-9-Signaling in ILC2s erforderlich für ihre Rekrutierung ins Lungengewebe und schützte die Zellpopulation autokrin durch Hochregulation des antiapoptotischen Proteins BCL-3 vor vorzeitigem Zelltod (Turner et al. 2013).

Der IL-9-Rezeptor konnte aber auch auf nicht-hämatopoetischen Zellen nachgewiesen werden. Gerlach et al. (2014) wiesen eine Hochregulation des IL-9-Rezeptors auf intestinalen Mucosazellen von Patienten nach, welche an Colitis ulcerosa oder Morbus Crohn erkrankt waren. Eine transiente Expression des Rezeptors konnte im Neokortex von Mäusen postnatal nachgewiesen werden (Fontaine et al., 2008). Zwischen Tag eins und zehn postnatal wurde der Rezeptor hochreguliert auf Neuronen nachgewiesen. Das Signaling verhinderte die Apoptose der Neuronen im Neokortex zu einem Zeitpunkt, wo massiv Neuronen durch programmierten Zelltod abgebaut werden (Fontaine et al, 2008).

Auf humanen bronchialen glatten Muskelzellen wurde ebenfalls der IL-9-Rezeptor nachgewiesen (Gounni et al., 2004). In Biopsien aus Bronchialgewebe von Asthma-Patienten konnte eine Erhöhung der Rezeptordichte gezeigt werden. Die Stimulation der Zellen *in vitro* mit IL-9 führte zur Ausschüttung von Eotaxin1/CCL11, welches chemotaktisch auf eosinophile Granulozyten wirkt. Auch auf humanem respiratorischen Epithel wurde der IL-9-Rezeptor beobachtet (Louahed et al, 2000). Insofern sind sowohl Immun- als auch Parenchymzellen Zielzellen von IL-9.

Die Funktion von IL-9 in Wurminfektionen und atopischen Erkrankungen

Einer der ersten Berichte über die Funktion von IL-9 zeigte seinen Einfluss bei der Bekämpfung von Fadenwürmern im Darm. So führte eine frühe Expression von IL-9 bei muriner Infektion mit Nematoden wie *T. muris* zu intestinaler Mastozytose und Produktion der Immunglobuline IgE und IgG1-Isotypen (Faulkner et al., 1998). Transgene IL-9-Mäuse waren besonders effektiv bei der Bekämpfung der Würmer. Die Parasiteninfektion geht typischerweise mit einer T_H2-Antwort einher, sodass IL-9 zunächst neben IL-4, IL-5 und IL-13 zu den T_H2-Zytokinen gezählt wurde.

Passend dazu wurde IL-9 bereits mit der Pathogenese atopischer Erkrankungen in Verbindung gebracht. In Bronchialbiopsien aus Patienten mit Asthma lag signifikant mehr IL-9 vor als in Biopsien von Patienten mit anderen Lungenerkrankungen wie chronischer Bronchitis oder Sarkoidose (Shimbara et al., 2000). Dabei korrelierte die Menge an IL-9 mit der gemessenen Obstruktion und bronchialen Hyperreagibilität der Patienten.
Mäuse mit lungenspezifisch transgener Expression von IL-9 zeigten eine Hyperreagibilität in den Bronchien, erhöhte IgE-Produktion, Immunzellinfiltration von Lymphozyten und Eosinophilen, Mastzell-Hyperplasie und subepitheliale Kollagenablagerung in der Lunge (Temann et al., 1998 und 2002). Hierbei konnte eine signifikante Induktion der T_H2-Zytokine IL-4, IL-5 und IL-13 gemessen werden. Die Blockade von IL-9 in einem murinen Modell für Asthma führte zu einem verbesserten klinischen Outcome sowie geringerer Inflammation (Cheng et al., 2002).

IL-9 im immunvermittelten Gewebeschaden

In der Infektion mit dem Parasiten *Nippostrongylus brasiliensis* konnten ILC2s als Hauptproduzent von IL-9 in der Lunge identifiziert werden (Turner et al., 2013). Wie oben erwähnt war IL-9 für die autokrine Stimulation der ILC2s notwendig. Die ILC2s produzierten IL-5, IL-13 und Amphiregulin, wodurch sie die Entwicklung eines Lungenemphysems *post infectionem* vermindern konnten (Turner et al., 2013).
Dahingegen zeigten Gerlach et al. (2014) in einem murinen Modell der humanen Colitis ulcerosa - der Oxazolon-Colitis (OC) -, dass IL-$9^{-/-}$-Mäuse einen geringeren Gewichtsverlust, Inflammation des Colons und Krankheitsaktivität im Vergleich zum Wildtyp (WT) aufwiesen. Dies beruhte auf einem direkten Effekt auf die Mucosa, welche durch Aktivierung des IL-9-Rezeptors vermehrt das kanalbildende Protein Claudin-2 und vermindert die barriereförderndern Proteine Claudin-3 und Occludin exprimierten. Dadurch wurde die Darmbarriere durch IL-9 geschwächt und die Infiltration kommensaler Bakterien gefördert. Nach Applikation eines IL-9-Antikörpers in erkrankte WT-Mäuse konnte dieser Effekt revidiert werden (Gerlach et al, 2014). Durch eine mittels Pinzette zugefügte Darmverletzung *in vivo* konnte nachgewiesen werden, dass IL-$9^{-/-}$-Mäuse eine verbesserte Wundheilung aufweisen als der Wildtyp. Der Effekt konnte durch rektale Gabe von IL-9 zusätzlich aggraviert werden (Gerlach et al., 2014). Insofern gibt es organ- und modellspezifisch sowohl proentzündliche als auch gewebsprotektive Eigenschaften.

IL-9 im Kontext von Nierenerkrankungen

Durch Eller et al. (2011) wurde im Modell der nephrotoxischen Serumnephritis (NTS) dargelegt, dass durch T_{reg}-Zellen (Tregs) produziertes IL-9 Mastzellen in die renalen Lymphknoten rekrutiert werden, welche den inflammatorisch induzierten Nierenschaden supprimieren. Dem gegenüber steht die Beobachtung, dass *in vitro* der sog. Mastertranskriptionsfaktor der T_{reg}-Zellen - Foxp3 - das IL-9-Gen durch Rekrutierung von Histondeacetylasen supprimiert (Xiao et al, 2015). *Ex vivo* isolierte Tregs naiver Mäuse produzieren kein IL-9, jedoch IL-9R mRNA (Elyaman et al., 2009). Die Aktivierung von GITR auf in vitro differenzierte iTregs bewirkt jedoch die Suppression von Foxp3 und aktiviert das IL-9-Gen (Xiao et al., 2015; Lu et al., 2006). Insofern ist denkbar, dass die GITR-Aktivierung essentiell für die IL-9-Produktion in Tregs ist.

In einem Modell akuten Nierenschadens durch das Zytostatikum Cisplatin wurde gezeigt, dass IL-9 in Sera und Nieren erkrankter Mäuse erniedrigt ist (Jiang et al, 2020). Durch Überexpression von IL-9 sanken die Nierenfunktionsparameter, inflammatorische Zytokine wie IL-6 und TNF- α sowie KIM-1, ein Biomarker für Schäden am proximalen Tubulus. Auch die Infiltration von Makrophagen ins Nierenparenchym sank. Die Autoren konnten durch Ko-Kultur differenzierter Makrophagen aus mit IL-9 vorbehandelten THP-1 Zellen mit HK-2-Zellen (entsprechend proximaler Tubuluszellen) trotz Cisplatin-Gabe eine Erniedrigung des KIM-1-Markers feststellen. THP-1-Zellen, welche mit IL-9 behandelt wurden, produzierten weniger TNF-α und IL-6, sodass die Autoren auf eine immunsuppressive Wirkung von IL-9 auf Makrophagen schlossen (Jiang et al, 2020).

Hypothese

In der Adriamycin-Nephropathie sind $CD4^+$-Zellen als protektiv beschrieben worden (Wang et al., 2004). In der Niere wurde IL-9 in zwei Modellen bereits als nephroprotektiv beschrieben (Eller at al., 2011; Jiang et al., 2020). Darauf beruhend stellten wir die Hypothese auf, dass IL-9 durch Aktivierung einer T_H2-Immunantwort oder Hochregulation von ILC2s den Nierengewebeschaden in der AN begrenzt.

IL-9 schützt vor progressiver Glomerusklerose und Nierenversagen in der Adriamycin-induzierten Nephropathie

Durch die intravenösen Injektion des Zytostatikums Adriamycin in jeweils Balb/c-Wildtyp (WT) und IL-9-Knockout (IL-9 $^{-/-}$) Mäuse wurde die Adriamycin-induzierte Nephropathie (AN) ausgelöst. Die laborchemische Analyse des Urins nach sieben Tagen nach Injektion zeigte eine signifikant erhöhte Albumin/Kreatinin-Ratio bei den IL-9-depletierten Mäusen im Vergleich zu der WT-Variante an (Abb. 1a). Im zeitlichen Verlauf glichen sich die Proteinuriewerte beider Gruppen an. Es zeigten sich keine signifikanten Unterschiede im Cholesterol, einem laborchemischen Parameter des nephrotischen Syndroms (Abb. 1e). Die histopathologische Evaluation der Glomerulosklerose an Tag 14 zeigte signifikant mehr sklerosierte Glomeruli in den Nieren der IL-9 $^{-/-}$ an, während der tubulointerstielle Schaden zwischen den Vergleichsgruppen keinen Unterschied zeigte (Abb. 1b, c). An Tag sieben stellen sich die Nieren beider Gruppen lichtmikroskopisch unauffällig dar. Passend zu den histopathologischen Ergebnissen waren die Harnstoffparameter im Urin bei den IL-9 $^{-/-}$-Mäusen an Tag 14 ebenfalls signifikant erhöht im Vergleich zur WT-Gruppe (Abb. 1d)
Zusammenfassend wurde dargelegt, dass IL-9-Defizienz im frühen Stadium der Erkrankung zu erhöhter Proteinurie führt, verursacht durch eine aggravierte Glomerulosklerose, welche zu Nierenfunktionsschäden im Verlauf führt.

IL-9-Defizienz hat keinen Einfluss auf die Immunzellinfiltration in der Niere sowie den Treg-Phänotyp in Nieren und renalen Lymphknoten bei Induktion der AN

Es ist erwiesen, dass Immunzellen bei der Pathogenese von CKDs eine wichtige Rolle spielen. Dass durch die AN-Induktion eine Immunzellinfiltration in die Niere erfolgt, wurde durch

Wang et al. 2000 bereits beschrieben. Da IL-9 auf mehrere verschiedene Immunzelltypen einen Einfluss haben kann, wurde die Immunzellinfiltration in die Niere zunächst durch Durchflusszytometrie untersucht. Hierbei zeigte sich zwischen der WT- und IL-9 $^{-/-}$-Gruppe nach Induktion der AN kein signifikanter Unterschied bei der Anzahl der Gesamtleukozyten, $CD4^+$- und $CD8^+$-T-Zellen sowie Tregs und ILC2s (Supplement 1A und 1B). Immunzellen der myeloischen Reihe wie Neutrophile, Eosinophile oder Makrophagen verhielten sich zwischen beiden Gruppen ebenfalls gleich (Suppl. 1A und 1B).

Nach Analyse der quantitativen Verhältnisse wurden die Treg-Zellen näher charakterisiert, da Tregs von IL-9$^{-/-}$ -Mäusen weniger koinhibitorische Proteine wie den glukokortikoid-induzierenden Tumornekrosefaktor (GITR) und induzierbaren T-Zell-Kostimulator (ICOS) exprimieren (Rauber et al., 2017). In diesem Zusammenhang zeigte sich bei IL-9 $^{-/-}$-defizienten Tregs eine erniedrigte immunsuppressive Kapazität mit überschießender Immunantwort im Mausmodell der Glomerulonephritis (Eller et al., 2011) und rheumatoider Arthritis (Rauber et al., 2017). Die Aktivierung von GITR auf in vitro differenzierte iTregs bewirkt die Suppression von Foxp3 und aktiviert das IL-9-Gen (Xiao et al., 2015). In unseren Analysen zeigten isolierte Tregs aus Niere und renalem Lymphknoten sowohl an Tag 14 nach AN-Induktion als auch in naiven Mäusen keine signifikanten Unterschiede bei der Expression von GITR, ICOS sowie PD-1 (Suppl. 2A and B)

Es zeigten sich zusammenfassend keine quantitativen Unterschiede der Immunzellinfiltration sowie beim Treg-Phänotyp in der Niere und renalem Lymphknoten nach AN-Induktion.

IL-9 hat keinen protektiven Effekt im Modell der nephrotoxischen Nephritis

Die Wirkung von IL-9 in einem Modell mit immunologisch induziertem Nierenschadens wurde mittels der nephrotoxischen Nephritis (NTN) untersucht. Hierzu wurde nephrotoxisches Serum aus Schafen mit IgG-Antikörpern gegen das Glomerulum Mäusen gespritzt (nach Panzer et al., 2007). Es zeigten sich bis auf signifikant erhöhte Serumharnstoffwerte in den Mäusen ohne IL-9 keine Unterschiede hinsichtlich der Histopathologie und dem Urinalbumin zwischen WT und IL-9$^{-/-}$-Gruppe (Suppl. 3A-D).

IL-9 schützt im frühen Stadium der AN Podozyten vor Zellschaden

Da sich lichtmikroskopisch kein Korrelat für die signifikant erhöhten Proteinurie-Werte an Tag sieben der AN bei der IL-9$^{-/-}$ -Gruppe zeigte, wurden die Nieren elektronenmikroskopisch

untersucht. Hierbei zeigten die Podozyten der IL-$9^{-/-}$-Mäuse an Tag sieben nach AN-Induktion im Vergleich zur WT-Gruppe signifikant mehr Verschmelzungen der Fußfortsetze (Abb. 2a, b), ein typisches Korrelat für Nierenerkrankungen mit Proteinurie. Immunhistochemisch zeigte sich an Tag sieben zusätzlich eine quantitativ niedrigere Podozytenzahl bei der IL-$9^{-/-}$ -Gruppe (Abb. 2c, d). Die Nieren beider Gruppe stellen sich naiv (d.h. ohne Induktion der Krankheit) mit den genannten Methoden unauffällig dar, sodass diese Daten auf einen direkten Zusammenhang zwischen IL-9 und Podozytenschaden im frühen Stadium der AN hinweisen.

T-Zellen und ILCs sind die Hauptproduzenten von IL-9 im AN-Modell

Zur Identifizierung der zellulären Quellen von IL-9 wurde die AN in *Il9^{Cre}R26R^{tdtomato}* „fate reporter"-Mäuse induziert (nach Wilhelm et al, 2011). Die Zellen dieser Mäuse produzieren nach Expression von IL-9 ein fluoreszierendes td-tomato-Protein, welches die Zellen permanent markiert. Immunhistochemisch konnten in den Nieren naiver und AN-erkrankter fate-reporter-Mäuse tomato-positive (IL-9^{fm+}) Zellen im Bereich der Glomeruli, tubulointerstitiell und perivaskulär detektiert werden (Abb. 3a). Durchflusszytometrisch waren unter 0.4 % der Leukozyten in beiden Gruppen konstant positiv für IL-9^{fm+} (Abb. 3b). Zellen der myeloischen Reihe sowie CD45-negative nicht-hämatopoetische Zellen zeigten fast keine Expression von IL-9^{fm+} (Suppl. Abb. 4A). Auch systemisch – d.h. im Blut oder in der Milz – zeigte sich keine wesentliche Anzahl an IL-9^{fm+}-positiven Zellen (Supplement Abb. 4B, C). Die Analyse der IL-9^{fm+}-positiven Leukozyten zeigte, dass vor allem ILCs und $CD4^+$-T-Zellen IL-9 produzieren (Abb. 3c, d). Quantitativ sowie im Verhältnis der produzierenden Zellen zeigte sich kein Unterschied zwischen naiven und kranken Mäusen (Abb. 3 a-d).

Naive $CD4^+$-T-Zellen lassen sich *in vitro* durch Stimulation des T-Zell-Rezeptors (TCR) und Hinzufügen der Zytokine TGF-β, IL-4, IL-6 und IL-1β zur IL-9-Produktion anregen (Veldhoen et al., 2008) und werden in der Literatur auch „T_H 9"-Zellen genannt. Dies ließ sich auch bei Isolation muriner $CD4^+$-Effektor-Zellen aus der Niere *in vitro* reproduzieren (Suppl. 5B).

Obwohl sich die Quantität der produzierenden IL-9-Zellen durch Induktion der Nephropathie nicht veränderte, konnte nach Isolation von Effektor-T-Zellen aus der Niere *in vivo* eine Hochregulation von TGF-β-, IL-1b- und IL-6-mRNA bei AN-erkrankten Mäusen im Vergleich zu naiven Mäusen nachgewiesen werden (Suppl. 5C), sodass eine T-Zell-Aktivierung durch residente Zellen ein möglicher Stimulus für die IL-9-Produktion in diesem Modell sein könnte.

IL-9-Expression aus dem adaptiven Immunsystem ist essenziell für den protektiven Effekt in der AN

Da ILCs prozentual den größten Anteil an IL-9^{fm+}-Zellen in der Niere darstellten (Abb. 3c), wurde die Hypothese aufgestellt, dass IL-9 aus dem angeborenen Immunsystem essenziel für den Schutz vor Glomerulosklerose ist. Hierfür wurden $Rag2^{-/-}$-Mäuse, welche aufgrund eines Enzymknockouts nicht imstande sind T- und B-Zellen auszureifen, mit IL-$9^{-/-}$-Mäusen zu IL-$9^{-/-}$$Rag2^{-/-}$-Mäusen gekreuzt. Diese Mäuse verfügen über kein funktionierendes adaptives Immunsystem und sind zusätzlich IL-9-defizient. Daraufhin wurde der Krankheitsverlauf AN-erkrankter IL-$9^{-/-}$$Rag2^{-/-}$-Mäuse mit $Rag2^{-/-}$-Tieren verglichen, welche zur IL-9-Produktion noch fähig sind (Abb. 4). Die Zellen des angeborenen Immunsystems, d.h. auch ILCs, sind in beiden Gruppen noch vorhanden. Zwischen beiden Gruppen zeigte sich kein Unterschied bei den laborchemischen Nierenfunktionsparametern und der Glomerulosklerose (Abb. 4a–e). Hierdurch konnte der Rückschluss gezogen werden, dass IL-9 aus dem adaptivem Immunsystem essenziell für den protektiven Effekt im Verlauf der AN ist.

IL-9 schützt Podozyten vor dem durch Adriamycin induzierten Zelltod

In der Literatur wird IL-9 als hauptsächlich auf Immunzellen wirkend beschrieben, es gibt jedoch auch Hinweise auf einen direkten Effekt auf residente Gewebszellen (siehe Einleitung). Da wir in diesem Modell keinen signifikanten Effekt des IL-9-Knockouts auf die Immunzellantwort messen konnten (Supp. 1), wurde ein direkter Effekt auf die renalen Epithelzellen der Niere in Betracht gezogen. Für diese Hypothese wurde zunächst die Expression des IL-9-Rezeptors (IL-9R) in isolierten murinen Glomeruli und im Tubulointerstitium anhand real-time PCR (rt-PCR) untersucht. Hier zeigte sich in beiden Kompartimenten die Expression von IL-9R-mRNA, wobei die Expression in den Glomeruli signifikant höher war als im Tubulointerstitium (Abb. 5a). Auch die Glomeruli AN-erkrankter Mäuse zeigten eine stete Expression von IL-9R-mRNA über den Verlauf der Erkrankung (Abb. 5b). Durch Immunfluoreszenzfärbung konnte *in vivo* die Expression des IL-9-Rezeptors auf Podozyten nachgewiesen werden (Abb. 5d); im geringeren Ausmaße fand sich der IL-9-Rezeptor auch auf glomerulären Endothelzellen.

Da Adriamycin apoptotisch auf die Podozyten wirkt, wurde *in vitro* eine murine Podozytenzelllinie auf die Expression von IL-9R hin untersucht. Auch diese Zellen zeigten in

der rt-PCR-Analyse die Expression von IL-9-mRNA (Abb 5c). Nach vorheriger Inkubation der Zellkulturen mit IL-9 in steigenden Konzentrationen erfolgte die Zugabe von Adriamycin. Durchflusszytometrisch konnte der apoptotische Effekt des Adriamycins auf die murine Podozytenzellkultur nachgewiesen werden; Zellkulturen, welche vorher ab 50 ng/mL und mehr mit IL-9 inkubiert wurden, wiesen eine signifikant geringere Anzahl apoptotischer, Annexin-V-positiver Zellen in der Durchflusszytometrie auf, wenn auch die Apoptose nicht ganz aufgehoben wurde (Abb. 5e). Dies könnte ein Hinweis darauf sein, dass IL-9 durch direktes Signaling im Podozyten vor Apoptose durch Adriamycin schützt.

Überexpression von IL-9 schützt vor Glomerulosklerose und Nierenversagen

Zur Evaluation des Potenzials von IL-9 als therapeutische Option im AN-Modell wurde der sog. hydrodynamische Gentransfer (HGD) eingesetzt. Hierfür wurde ein nicht-viraler Plasmidvektor, welcher IL-9 codiert, schnell und mit viel Volumen in die Schwanzvene der Maus injiziert. Durch das hohe Volumen staut sich die applizierte Flüssigkeit zurück in die Hohlvene, sodass der Vektor hauptsächlich von der Leber aufgenommen wird. Drei Tage nach Transfektion erfolgte die Injektion von Adriamycin. Mäuse, welche mit dem IL-9-Vektor behandelt wurden, zeigten im Vergleich zur Kontrollvektor-behandelten Gruppe einen signifikanten Anstieg von IL-9 im Serum (Abb. 6a). Mit IL-9-Vektor behandelte Mäuse zeigten auch niedrigere Albumin-Werte im Urin, wenn auch nicht signifikant (Abb. 6b). Auffällig sind die signifikant niedrigeren Harnstoff- und Cholesterinwerte, sowie die stark reduzierte Glomerulosklerose in der IL-9-Vektor-Gruppe (Abb. 6c-f). Auch quantitativ wurden mehr Podozyten pro Glomerulus in der IL-9-Vektor-Gruppe gemessen (Abb. 6g). Diese Daten weisen darauf hin, dass eine IL-9-Überexpression *in vivo* dem AN-Verlauf mit Glomerulosklerose, nephrotischem Syndrom und Nierenversagen erheblich entgegenwirkt.

IL-9 ist im Serum von Patient:innen mit fokal-segmentaler Glomerulosklerose (FSGS) erhöht

Um zu sehen, ob unsere Ergebnisse von Relevanz für den Menschen sein könnten, wurden Blutseren von Patient:innen mit fokal segmentaler Glomerulosklerose (FSGS) (n = 14) mit gesunden Kontrollen (n = 14) verglichen. Für den Menschen stellt die FSGS das histopathologische Korrelat zur murinen AN dar; ähnlich zur AN weisen die Patient:innen auch ein nephrotisches Syndrom auf. Mit Hilfe eines hochsensiblen Immunassays wurde in beiden

Gruppen IL-9 im Serum detektiert; die Patienten mit FSGS wiesen jedoch ein signifikant höheres Level auf (Abb. 7), was auf eine Hochregulation im Rahmen des Nierenschadens hinweist. Die IL-9-Level korrelierten in dieser kleinen Kohorte nicht mit dem Ausmaß der Proteinurie oder des Kreatinins.

Diskussion

In der hier vorliegenden Arbeit wurde aufgezeigt, dass eine IL-9-Defizienz im Gegensatz zum Wildtyp in der murinen Adriamycin-Nephropathie (AN) durch eine aggravierte Glomerulosklerose auffällt. Als Mechanismus wurde nach Nachweis des IL-9-Rezeptors auf Podozyten und *in vitro*-Experimenten festgestellt, dass IL-9 direkt antiapoptotisch auf Podozyten wirkt. Im Laufe der Erkrankung zeigten sich keine Unterschiede bei der Immunzellinfiltration in die Niere; ILC2s und T-Zellen konnten jedoch als Hauptproduzenten von IL-9 in der Niere identifiziert werden. Für den Phänotyp relevant waren unseren Ergebnissen nach die $CD4^+$-T-Zellen. Eine systemische Überexpression von IL-9 verhinderte die Glomerulosklerose, was effektiv zu einem verbesserten Outcome der Nierenfunktion führte. IL-9 wurde bisher wenig hinsichtlich seiner Wirkung auf residente Zellen und Apoptose hin untersucht. *In vitro* nachgezüchtete Colonkrypten in Form von sog. Organoiden zeigten nach Gabe von IL-9 keinen Effekt hinsichtlich der Apoptose (Gerlach et al., 2014), die Zellproliferation zeigte sich jedoch erniedrigt. IL-9 bewahrt durch Hochregulation von BCL-3 ILC2s vor dem vorzeitigen Zelltod (Wilhelm et al., 2012). Respiratorische Epithelzellen durchliefen nach Gabe von IL-9 *in vitro* weniger Apoptose, was mit einer Hochregulation des antiapoptotischen Moleküls BCL-2 assoziiert war (Singhera et al., 2008). Im Kontext einer Entzündung, wie es bei Asthma der Fall ist, triggert IL-9 jedoch die Inflammation im respiratorischen Gewebe (siehe Einleitung). Dies deutet auf eine kontext- und organspezifische Wirkung von IL-9 hin. Wir wiesen im Rahmen eines nicht-inflammatorisch vermittelten Gewebeschadens eine antiapoptotische Wirkung von IL-9 auf Podozyten nach.

Eine direkte Detektion von IL-9 oder IL-9-mRNA ließ sich aufgrund des geringen Niveaus mit den zur Verfügung stehenden Methoden nicht zuverlässig erreichen. Eine Hochregulation IL-9-produzierender Zellen war nicht zu verzeichnen. Zu diskutieren ist eine mögliche Hochregulation von IL-9 in den residenten Immunzellen der Niere. So produzierten *in vitro* isolierte $CD4^+$-Zellen aus der Niere vermehrt IL-9 nach T-Zell-Rezeptor-Aktivierung und Stimulation mit bestimmten Zytokinen, welche im Rahmen der AN hochreguliert in der Niere nachweisbar waren (Supp. 5C).

Nicht untersucht wurde die Funktionsfähigkeit des Immunzellkompartments; so zeigten z.B. aus $IL\text{-}9^{-/-}$-Mäusen isolierte T_{reg}-Zellen in einem Arthritis-Modell eine geringere Fähigkeit zur Immunsuppression (Rauber et al., 2017). Die Zellen wiesen jedoch eine auch eine geringere Expression der Effektormoleküle ICOS und GITR auf, was in unseren Experimenten nicht der Fall war (Supp. 2A und B). Auch wenn eine Immunzellinfiltration in die Niere in der AN stattfindet, ist sie zu dem Zeitpunkt, wo bereits ein deutlicher Unterschied im Podozytenschaden

nachweisbar ist, nur gering (Wang et al., 2000). Wir halten daher eine zwischengeschaltete Immunantwort als Erklärung für den Phänotyp für unwahrscheinlich.

Möglich ist auch ein homöostatischer Effekt von IL-9 auf die Podozyten, welcher bis zu einem gewissen Ausmaß die Podoyzten vor z.B. oxidativem Stress schützt. Diese Hypothese eines endogenen Effektes wird gestützt durch die Beobachtung, dass die Behandlung von IL-$9^{-/-}$-Mäusen mit IL-9 intraperitoneal nicht antiapoptotisch auf Neuronen wirkte, bei WT-Mäusen aber schon (Fontaine et al., 2008). Wie auf Signaling-Ebene IL-9 die Apoptose im Podozyten verhindert, war nicht Teil der Studie und ist daher in Zukunft noch zu klären.

In vitro waren im Gegensatz zu den *in vivo*-Experimenten höhere Dosen von IL-9 notwendig, um die Podozyten vor Apoptose zu schützen. Wir führten diese Diskrepanz auf eine unterschiedliche Rezeptor-Expression und Ansprechen des Zytokins auf die immortalisierte Podozytenzelllinie zurück. Der IL-9-Rezeptor war zusätzlich auf den Endothelzellen des Glomerulus nachweisbar (Abb. 5c), sodass diese möglichweise zur Nephroprotektion beitragen.

Was für eine Rolle IL-9 bei chronischen Nierenerkrankungen im Menschen spielt, ist noch unklar. Bei Patienten, welche an einer Pauci-immunen fokal-segmentalen nekrotisierenden Glomerulonephritis (FSNGN) erkrankt waren, war eine erhöhte IL-9-Detektion im Urin assoziiert mit einem verbesserten Outcome nach immunsuppressiver Therapie (Stangou et al., 2011). Nach Transplantation humaner Nieren konnte eine direkte Ausschüttung von IL-9 aus Organen festgestellt werden, welche post mortem entnommen wurden. Diese waren anfälliger für die Entwicklung eines Reperfusionsschadens im Gegensatz zu Nieren aus Lebendspenden (Kortekaas et al., 2013). Wir konnten im Serum FSGS-erkrankter Patienten erhöhte IL-9-Spiegel messen. Eine Korrelation zu klinischen Funktionsparametern konnte aufgrund der kleinen Kohorte nicht bestimmt werden, sodass weitere Studien hierzu notwendig sind.

Die systemische Überexpression von IL-9 zeigte in unserer Arbeit ein deutlich verbessertes Outcome in der AN. Die subkutane Applikation von IL-9 über 40 Tage führte in der Niere von Mäusen zu Kollagenablagerungen und dosisabhängig zu Lymphozyteninfiltration (de Lira Silva et al., 2019). Zusätzlich gibt es Berichte über eine Assoziation von IL-9 mit der Bildung atheroskletorischer Ablagerungen in der Maus (Li et al., 2017) sowie im Menschen (Gregersen et al., 2013). Insofern ist IL-9 als therapeutische Option aufgrund des Zusammenhanges zwischen chronischen Nieren- und kardiovaskulären Erkrankungen mit erhöhter Mortalität noch sorgfältig zu untersuchen.

3. Literaturverzeichnis

Angkasekwinai P, Dong C. IL-9-producing T cells: potential players in allergy and cancer. Nat Rev Immunol. Januar 2021;21(1):37–48.

Barbey MM, Fels LM, Soose M, Poelstra K, Gwinner W, Bakker W, u. a. Adriamycin affects glomerular renal function: evidence for the involvement of oxygen radicals. Free Radic Res Commun. 1989;7(3–6):195–203.

Chang YT, Wu JL, Hsu CC, Wang JD, Sung JM. Diabetes and end-stage renal disease synergistically contribute to increased incidence of cardiovascular events: a nationwide follow-up study during 1998-2009. Diabetes Care. 2014;37(1):277–85.

Chen TK, Knicely DH, Grams ME. Chronic Kidney Disease Diagnosis and Management: A Review. JAMA. 1. Oktober 2019;322(13):1294–304.

Cheng G, Arima M, Honda K, Hirata H, Eda F, Yoshida N, u. a. Anti–Interleukin-9 Antibody Treatment Inhibits Airway Inflammation and Hyperreactivity in Mouse Asthma Model. Am J Respir Crit Care Med. 1. August 2002;166(3):409–16.

de Lira Silva NS, Borges BC, da Silva AA, de Castilhos P, Teixeira TL, Teixeira SC, u. a. The Deleterious Impact of Interleukin 9 to Hepatorenal Physiology. Inflammation. August 2019;42(4):1360–9.

Eller K, Wolf D, Huber JM, Metz M, Mayer G, McKenzie ANJ, u. a. IL-9 production by regulatory T cells recruits mast cells that are essential for regulatory T cell-induced immune suppression. J Immunol. 1. Januar 2011;186(1):83–91.

Elyaman W, Bradshaw EM, Uyttenhove C, Dardalhon V, Awasthi A, Imitola J, u. a. IL-9 induces differentiation of TH17 cells and enhances function of FoxP3+ natural regulatory T cells. Proceedings of the National Academy of Sciences. 4. August 2009;106(31):12885–90.

Faulkner H, Renauld JC, Van Snick J, Grencis RK. Interleukin-9 Enhances Resistance to the Intestinal Nematode *Trichuris muris*. Infect Immun. August 1998;66(8):3832–40.

Fogo AB. Causes and pathogenesis of focal segmental glomerulosclerosis. Nat Rev Nephrol. Februar 2015;11(2):76–87.

Fontaine RH, Cases O, Lelièvre V, Mesplès B, Renauld JC, Loron G, u. a. IL-9/IL-9 receptor signaling selectively protects cortical neurons against developmental apoptosis. Cell Death & Differentiation. Oktober 2008;15(10):1542–52.

Gerlach K, Hwang Y, Nikolaev A, Atreya R, Dornhoff H, Steiner S, u. a. TH9 cells that express the transcription factor PU.1 drive T cell-mediated colitis via IL-9 receptor signaling in intestinal epithelial cells. Nat Immunol. Juli 2014;15(7):676–86.

Goswami R, Kaplan MH. A Brief History of IL-9. J Immunol. 15. März 2011;186(6):3283–8.

Gounni AS, Hamid Q, Rahman SM, Hoeck J, Yang J, Shan L. IL-9-Mediated Induction of Eotaxin1/CCL11 in Human Airway Smooth Muscle Cells. The Journal of Immunology. 15. August 2004;173(4):2771–9.

Gregersen I, Skjelland M, Holm S, Holven KB, Krogh-Sørensen K, Russell D, u. a. Increased Systemic and Local Interleukin 9 Levels in Patients with Carotid and Coronary Atherosclerosis. PLoS One. 30. August 2013;8(8):e72769.

Guo J, Ananthakrishnan R, Qu W, Lu Y, Reiniger N, Zeng S, u. a. RAGE mediates podocyte injury in adriamycin-induced glomerulosclerosis. J Am Soc Nephrol. Mai 2008;19(5):961–72.

Hültner L, Druez C, Moeller J, Uyttenhove C, Schmitt E, Rüde E, u. a. Mast cell growth-enhancing activity (MEA) is structurally related and functionally identical to the novel mouse T cell growth factor P40/TCGFIII (interleukin 9). Eur J Immunol. Juni 1990;20(6):1413–6.

Jäger A, Dardalhon V, Sobel RA, Bettelli E, Kuchroo VK. Th1, Th17, and Th9 Effector Cells Induce Experimental Autoimmune Encephalomyelitis with Different Pathological Phenotypes. The Journal of Immunology. 1. Dezember 2009;183(11):7169–77.

Jiang W, Yuan X, Zhu H, He C, Ge C, Tang Q, u. a. Inhibition of Histone H3K27 Acetylation Orchestrates Interleukin-9-Mediated and Plays an Anti-Inflammatory Role in Cisplatin-Induced Acute Kidney Injury. Front Immunol. 3. März 2020;11:231.

Kortekaas KA, de Vries DK, Reinders MEJ, Lievers E, Ringers J, Lindeman JHN, u. a. Interleukin-9 release from human kidney grafts and its potential protective role in renal ischemia/reperfusion injury. Inflamm Res. Januar 2013;62(1):53–9.

Lee VW, Harris DC. Adriamycin nephropathy: A model of focal segmental glomerulosclerosis. Nephrology. 2011;16(1):30–8.

Li Q, Ming T, Wang Y, Ding S, Hu C, Zhang C, u. a. Increased Th9 cells and IL-9 levels accelerate disease progression in experimental atherosclerosis. Am J Transl Res. 15. März 2017;9(3):1335–43.

Louahed J, Toda M, Jen J, Hamid Q, Renauld JC, Levitt RC, u. a. Interleukin-9 Upregulates Mucus Expression in the Airways. Am J Respir Cell Mol Biol. Juni 2000;22(6):649–56.

Lu LF, Lind EF, Gondek DC, Bennett KA, Gleeson MW, Pino-Lagos K, u. a. Mast cells are essential intermediaries in regulatory T-cell tolerance. Nature. 31. August 2006;442(7106):997–1002.

Mock BA, Krall M, Kozak CA, Nesbitt MN, McBride OW, Renauld JC, u. a. IL9 maps to mouse chromosome 13 and human chromosome 5. Immunogenetics. 1990;31(4):265–70.

Narres M, Claessen H, Droste S, Kvitkina T, Koch M, Kuss O, u. a. The Incidence of End-Stage Renal Disease in the Diabetic (Compared to the Non-Diabetic) Population: A Systematic Review. PLoS One [Internet]. 26. Januar 2016 [zitiert 23. Mai 2021];11(1). Verfügbar unter: https://www.ncbi.nlm.nih.gov/pmc/articles/PMC4727808/

Panzer U, Steinmetz OM, Paust HJ, Meyer-Schwesinger C, Peters A, Turner JE, u. a. Chemokine receptor CXCR3 mediates T cell recruitment and tissue injury in nephrotoxic nephritis in mice. J Am Soc Nephrol. Juli 2007;18(7):2071–84.

Rauber S, Luber M, Weber S, Maul L, Soare A, Wohlfahrt T, u. a. Resolution of inflammation by interleukin-9-producing type 2 innate lymphoid cells. Nat Med. August 2017;23(8):938–44.

Rauber S, Luber M, Weber S, Maul L, Soare A, Wohlfahrt T, u. a. Resolution of inflammation by interleukin-9-producing type 2 innate lymphoid cells. Nat Med. August 2017;23(8):938–44.

Shimbara A, Christodoulopoulos P, Soussi-Gounni A, Olivenstein R, Nakamura Y, Levitt RC, u. a. IL-9 and its receptor in allergic and nonallergic lung disease: increased expression in asthma. J Allergy Clin Immunol. Januar 2000;105(1 Pt 1):108–15.

Singhera GK, MacRedmond R, Dorscheid DR. Interleukin-9 and -13 inhibit spontaneous and corticosteroid induced apoptosis of normal airway epithelial cells. Exp Lung Res. November 2008;34(9):579–98.

Stangou M, Papagianni A, Bantis C, Liakou H, Pliakos K, Giamalis P, u. a. Detection of multiple cytokines in the urine of patients with focal necrotising glomerulonephritis may predict short and long term outcome of renal function. Cytokine. Januar 2012;57(1):120–6.

Temann UA, Geba GP, Rankin JA, Flavell RA. Expression of Interleukin 9 in the Lungs of Transgenic Mice Causes Airway Inflammation, Mast Cell Hyperplasia, and Bronchial Hyperresponsiveness. Journal of Experimental Medicine. 5. Oktober 1998;188(7):1307–20.

Turner JE, Morrison PJ, Wilhelm C, Wilson M, Ahlfors H, Renauld JC, u. a. IL-9–mediated survival of type 2 innate lymphoid cells promotes damage control in helminth-induced lung inflammation. Journal of Experimental Medicine. 16. Dezember 2013;210(13):2951–65.

Uyttenhove C, Simpson RJ, Snick JV. Functional and structural characterization of P40, a mouse glycoprotein with T-cell growth factor activity. PNAS. 1. September 1988;85(18):6934–8.

Veldhoen M, Uyttenhove C, van Snick J, Helmby H, Westendorf A, Buer J, u. a. Transforming growth factor-β „reprograms“ the differentiation of T helper 2 cells and promotes an interleukin 9–producing subset. Nat Immunol. Dezember 2008;9(12):1341–6.

Wang Y, Wang YP, Tay YC, Harris DCH. Progressive adriamycin nephropathy in mice: Sequence of histologic and immunohistochemical events. Kidney International. Oktober 2000;58(4):1797–804.

Wang Y, Wang YP, Tay YC, Harris DCH. Role of CD8+ cells in the progression of murine adriamycin nephropathy. Kidney International. 1. März 2001;59(3):941–9.

Wang Y, Wang Y, Feng X, Bao S, Yi S, Kairaitis L, u. a. Depletion of CD4+ T cells aggravates glomerular and interstitial injury in murine adriamycin nephropathy. Kidney International. 1. März 2001;59(3):975–84.

Wilhelm C, Hirota K, Stieglitz B, Van Snick J, Tolaini M, Lahl K, u. a. An IL-9 fate reporter demonstrates the induction of an innate IL-9 response in lung inflammation. Nat Immunol.

November 2011;12(11):1071–7.

Wilhelm C, Turner JE, Van Snick J, Stockinger B. The many lives of IL-9: a question of survival? Nature Immunology. Juli 2012;13(7):637–41.

Xiao X, Shi X, Fan Y, Zhang X, Wu M, Lan P, u. a. GITR subverts Foxp3 + Tregs to boost Th9 immunity through regulation of histone acetylation. Nature Communications. 14. September 2015;6(1):8266.

Yasuda K, Park HC, Ratliff B, Addabbo F, Hatzopoulos AK, Chander P, u. a. Adriamycin Nephropathy. Am J Pathol. April 2010;176(4):1685–95.

Zhang L, Wu JH, Otto JC, Gurley SB, Hauser ER, Shenoy SK, u. a. Interleukin-9 mediates chronic kidney disease-dependent vein graft disease: a role for mast cells. Cardiovasc Res. 1. November 2017;113(13):1551–9.

4. Zusammenfassung / Summary

Die progressive Glomerulosklerose als Form der chronischen Nierenerkrankung stellt ein globales Gesundheitsproblem dar. Die murine Adriamycin-Nephropathie (AN) ist charakterisiert durch die Entwicklung eines nephrotischen Syndroms und histopathologischen Veränderungen, welche der humanen fokal segmentalen Glomerulosklerose (FSGS) ähneln. Die genauen pathologischen Hintergründe chronischen Nierenschadens sind komplex und nicht vollständig durchleuchtet. Interleukin 9 (IL-9), bekannt als regulierender Faktor von Typ 2-Zytokinen sowie Wachstumsfaktor verschiedener Immunzelltypen, wird vermehrt hinsichtlich seiner Funktion im immunvermittelten Gewebeschaden diskutiert.
In unserer Arbeit konnten wir zeigten, dass IL-$9^{-/-}$-Mäuse in der AN mit einer vermehrten Glomerulosklerose und damit einhergehend mit einem Nierenfunktionsverlust auffallen. Als Mechanismus wurde nach Nachweis des IL-9-Rezeptors auf Podozyten und *in vitro*-Experimenten festgestellt, dass IL-9 direkt antiapoptotisch auf Podozyten wirkt. Unterschiede in der Immunzellinfiltration lagen nicht vor; $CD4^{+}$-T-Zellen konnten als relevante IL-9-produzierende Zellen in diesem Modell identifiziert werden. Eine systemische Überexpression von IL-9 verbesserte das Outcome deutlich, sodass IL-9 potentiell eine therapeutische Option proteinurischer Nierenerkrankungen darstellt.

Progressive glomerulosclerosis as a form of chronic kidney disease is a global health burden. In particular, murine Adriamycin nephropathy (AN) shows development of nephrotic syndrome and histopathological changes reminiscent of human focal segmental glomerulosclerosis (FSGS). The underlying pathological mechanisms of chronic kidney disease are complex and not fully understood. Interleukin 9 (IL-9), known as an upstream regulator of type 2 cytokines as well as a growth- and survival factor of different immune cell subsets, has been put into the context of resolution of tissue injury in the recent years.
In our study, we show that IL-$9^{-/-}$-mice show a severe phenotype in AN having more glomerulosclerosis and impairment of kidney function. Podocyte damage was more pronounced during the early stages of AN. While the immune cell infiltration into kidney and spleen between WT and IL-$9^{-/-}$ was unaffected, we could show that the IL-9 receptor is expressed on podocytes *in vivo*. IL-9 directly decreased apoptosis in podocytes *in vitro*. $CD4^{+}$-T-lymphocytes were identified as the relevant source of IL-9 in this model. In addition, systemic overexpression of IL-9 protected from glomerulosclerosis and kidney failure. Therefore, IL-9 could possibly serve as a potential target in proteinuric kidney disease.

5. Erklärung des Eigenanteils

Das Konzept sowie das experimentelle Design der hier vorliegenden Arbeit wurden unter Federführung von PD Dr. Jan-Eric Turner in engem Austausch mit mir und Dr. Tingting Xiong erstellt.
Durchgeführt und ausgewertet wurden die Experimente zusammen mit Tingting Xiong: Tierexperimentelles Arbeiten (Stoffwechselkäfige, Organentnahme); Leukozytenisolation; Messungen und Zellsortierung via Durchflusszytometrie, ELISA (Albumin); realtime PCR; statistische Analysen. Alleine durchgeführt habe ich die histopathologische Auswertung der PAS-Schnitte AN-erkrankter Mäuse.
In Zusammenarbeit mit den Ko-Authoren wurde das endgültige Manuskript entworfen und von PD Dr. Jan-Eric Turner und Dr. Tingting Xiong geschrieben.

6. Danksagung

Mein Dank gilt:

Prof. Dr. T. Huber für die Möglichkeit, die Arbeit in der III. Medizinischen Klinik durchführen zu können.

PD Dr. Jan-Eric Turner für die Betreuung, Geduld und das Gewähren vieler Freiräume – vielen Dank.

Prof. Dr. U. Panzer für die Auswertung der NTN-crescents und Aufnahme in das Promotionsprogramm.

Dr. Tingting Xiong für die Übernahme und gewissenhafte Beendigung des Projektes sowie die nette Zusammenarbeit.

Dr. Martina Becker für die Offenbarung des FACS-Universums und sowieso Danke.

Dr. Ann-Christin Gnirck für ihre Hilfe, Unterstützung und fröhlichen Stunden im Labor.

Kerstin Kopp für die tolle Einarbeitung sowie Diskussionen fachlicher und nicht-fachlicher Natur.

Prof. Dr. C. Meyer-Schwesinger für die Isolation der Glomeruli und die tollen Bilder davon.

Malte Wunderlich und Constantin Rickassel für ihre Mitarbeit am Projekt.

Allen Ko-Autoren

Alexandra Elbakyan

Meiner Familie und Freunden für den mentalen Support.

7. Lebenslauf

Entfällt aus Datenschutzgründen

8. Eidesstattliche Versicherung

Ich versichere ausdrücklich, dass ich die Arbeit selbständig und ohne fremde Hilfe verfasst, andere als die von mir angegebenen Quellen und Hilfsmittel nicht benutzt und die aus den benutzten Werken wörtlich oder inhaltlich entnommenen Stellen einzeln nach Ausgabe (Auflage und Jahr des Erscheinens), Band und Seite des benutzten Werkes kenntlich gemacht habe.

Ferner versichere ich, dass ich die Dissertation bisher nicht einem Fachvertreter an einer anderen Hochschule zur Überprüfung vorgelegt oder mich anderweitig um Zulassung zur Promotion beworben habe.

Ich erkläre mich einverstanden, dass meine Dissertation vom Dekanat der Medizinischen Fakultät mit einer gängigen Software zur Erkennung von Plagiaten überprüft werden kann.

Unterschrift: